Nanodiamond-Rich Layer Across Three Continents Consistent with Major Cosmic Impact at 12,800 Cal BP

26 authors, including:

Some of the authors of this publication are also working on these related projects:

Zirahuen, Michoacan View project

Millennial-scale climate variability in the Pleistocene Pacific View project

ARTICLES

Nanodiamond-Rich Layer across Three Continents Consistent with Major Cosmic Impact at 12,800 Cal BP

Charles R. Kinzie,[1,*] *Shane S. Que Hee,*[2] *Adrienne Stich,*[1] *Kevin A. Tague,*[1]
Chris Mercer,[3] *Joshua J. Razink,*[4] *Douglas J. Kennett,*[5] *Paul S. DeCarli,*[6,†] *Ted E. Bunch,*[7]
James H. Wittke,[7] *Isabel Israde-Alcántara,*[8] *James L. Bischoff,*[9] *Albert C. Goodyear,*[10]
Kenneth B. Tankersley,[11] *David R. Kimbel,*[12] *Brendan J. Culleton,*[5] *Jon M. Erlandson,*[13]
Thomas W. Stafford,[14] *Johan B. Kloosterman,*[15] *Andrew M. T. Moore,*[16]
Richard B. Firestone,[17] *J. E. Aura Tortosa,*[18] *J. F. Jordá Pardo,*[19]
Allen West,[20,‡] *James P. Kennett,*[21] *and Wendy S. Wolbach*[1]

ABSTRACT

A major cosmic-impact event has been proposed at the onset of the Younger Dryas (YD) cooling episode at ≈12,800 ± 150 years before present, forming the YD Boundary (YDB) layer, distributed over >50 million km^2 on four continents. In 24 dated stratigraphic sections in 10 countries of the Northern Hemisphere, the YDB layer contains a clearly defined abundance peak in nanodiamonds (NDs), a major cosmic-impact proxy. Observed ND polytypes include cubic diamonds, lonsdaleite-like crystals, and diamond-like carbon nanoparticles, called n-diamond and i-carbon. The ND abundances in bulk YDB sediments ranged up to ≈500 ppb (mean: 200 ppb) and that in carbon spherules up to ≈3700 ppb (mean: ≈750 ppb); 138 of 205 sediment samples (67%) contained no detectable NDs. Isotopic evidence indicates that YDB NDs were produced from terrestrial carbon, as with other impact diamonds, and were not derived from the impactor itself. The YDB layer is also marked by abundance peaks in other impact-related proxies, including cosmic-impact spherules, carbon spherules (some containing NDs), iridium, osmium, platinum, charcoal, aciniform carbon (soot), and high-temperature melt-glass. This contribution reviews the debate about the presence, abundance, and origin of the concentration peak in YDB NDs. We describe an updated protocol for the extraction and concentration of NDs from sediment, carbon spherules, and ice, and we describe the basis for identification and classification of YDB ND polytypes, using nine analytical approaches. The large body of evidence now obtained about YDB NDs is strongly consistent with an origin by cosmic impact at ≈12,800 cal BP and is inconsistent with formation of YDB NDs by natural terrestrial processes, including wildfires, anthropogenesis, and/or influx of cosmic dust.

Online enhancements: appendixes.

Introduction

The Younger Dryas (YD) impact hypothesis proposes that a major cosmic-impact event occurred at the Younger Dryas Boundary (YDB) 10,900 ± 145 radiocarbon years before present (RCYBP), a time corresponding to the onset of the YD cooling recorded in Greenland Ice Sheet cores and other se-

quences (Firestone et al. 2007). The published IntCal radiocarbon curve has recently been revised (Reimer et al. 2013) and provides a calibrated age for this radiocarbon date of ≈12,830 ± 130 cal BP at 1 standard deviation (σ). This differs from earlier calibrated ages for the YDB of 12,900 ± 100 cal BP, used by Firestone et al. (2007), and 12,800 ± 150 cal BP, more recently used by Wittke et al. (2013). Because this latest adjustment represents a difference of only ≈30 yr, we continue to use an age of 12,800 ± 150 cal BP for the YDB. We emphasize that, although the calendar calibration has

changed, the radiocarbon age has remained the same.

The proposed impact deposited the YDB layer, which contains many cosmic-impact proxies, including magnetic and glassy impact spherules, iridium, fullerenes, carbon spherules, glass-like carbon, charcoal, and aciniform carbon, a form of soot (Firestone et al. 2007; Wittke et al. 2013). In North America and the Middle East, Bunch et al. (2012) identified YDB melt-glass that formed at high temperatures (1730° to >2200°C), as also reported by three independent groups, Mahaney et al. (2010) in South America and Fayek et al. (2012) and Wu et al. (2013) in North America. This study focuses solely on nanodiamonds (NDs), and so, for independent discussions of other proxies, see Haynes et al. (2010) and Paquay et al. (2009), who found no evidence for the platinum-group elements iridium or osmium. Alternately, Wu et al. (2013) found large YDB anomalies in osmium, as discussed below. Also, in a Greenland ice core, Petaev et al. (2013) found a large YDB abundance peak in the platinum-group element platinum. Surovell et al. (2009) found no YDB peaks in magnetic spherules, whereas LeCompte et al. (2012) found large, well-defined YDB spherule peaks at sites common to the study by Surovell et al. Also, critical overviews of the YDB hypothesis are presented in Pinter et al. (2011) and Boslough et al. (2012).

Recently, the YDB cosmic impact was independently confirmed by Petaev et al. (2013), who reported compelling evidence from a well-dated Greenland Ice Core Project (GISP2) ice core exhibiting a sharp abundance peak in platinum precisely at the YD onset (12,877 ± 3.4 cal BP). Those authors' mass-balance calculations indicate that the platinum peak resulted from a major cosmic-impact event by an impactor estimated to be at least 1 km in diameter. Similarly, Wittke et al. (2013) estimated that the tonnage of YDB ejecta (spherules and melt-glass) is comparable to that ejected from the 10.5-km-wide Bosumtwi Crater, likely produced by a 1-km-wide impactor. The GISP2 platinum peak is coeval with the abrupt onset (≈1.5 yr) of the atmospheric changes that mark the YD climatic episode in the North Greenland Ice Core Project (NGRIP) ice core at 12,896 cal BP (Steffensen et al. 2008). The discovery of such an unequivocal impact proxy at the YD onset in the Greenland record was predicted by the YDB impact hypothesis when it was initially introduced (Firestone et al. 2007).

The comprehensive impact proxy assemblage in the YDB layer also includes NDs and diamond-like carbon, which were discovered within carbon spherules, glass-like carbon, and bulk sediment. The polymorphs of carbon extracted from bulk sediment and carbon spherules include cubic NDs and hexagonal lonsdaleite-like crystals as well as unique carbon allotropes, called n-diamonds and i-carbon (details in table D1; apps. A–D available online). These latter two types of nanocrystals, almost as hard as cubic NDs, are frequently used in thin, polycrystalline films for industrial applications requiring hardness and abrasion resistance (Wen et al. 2007). Ongoing investigations have been examining whether these polymorphs are simply cubic diamonds with atomic substitution of carbon by hydrogen or other elements (Wen et al. 2011) or are new forms of diamond-like carbon (Hu et al. 2012). Regardless, the nanoparticles in question form under exotic temperatures and pressures not present naturally at the Earth's surface or lower atmosphere but similar to conditions related to cosmic impact (Wen et al. 2007) and are unlike other forms of carbon typically found naturally on Earth. For simplicity, we refer to all forms as NDs, even though n-diamonds and i-carbon may actually be only diamond-like. YDB NDs were most likely formed from terrestrial carbon, based on their carbon isotopic composition (Tian et al. 2011; Israde-Alcántara et al. 2012b), and are similar to NDs formed during the cosmic impact at the Cretaceous-Paleogene boundary (K-Pg, formerly referred to as the K-T; Gilmour et al. 1992).

The YDB carbon spherules that contain NDs are morphologically and compositionally similar to younger carbon spherules first reported in near-surface forest soils of Europe by Rösler et al. (2005), who first suggested an impact-related origin of the particles. Later, some of the same authors (Yang et al. 2008) stated, "Whether this would have occurred during or before any impact is still unclear for now" (p. 943). Carbon spherules have been proven to form in cosmic-impact events, as shown by the discovery of a <1100-yr-old meteorite crater in Alberta, Canada (Newman and Herd 2013). Some carbon spherules are fused to fragments of the meteorite, indicating that they formed upon impact. Their morphology includes an exterior shell around a highly vesicular interior, identical to YDB spherules and carbon spherules found in Europe. Carbon spherules have also been reported from experiments using hypervelocity impacts into carbon-rich substrates, duplicating cosmic-impact conditions (Heymann et al. 2006). Furthermore, carbon spherules containing NDs have been demonstrated to form from tree sap under laboratory conditions

that duplicate the temperature, pressure, and redox values within an impact fireball (Israde-Alcántara et al. 2012b).

Following the identification of NDs by Kennett et al. (2009a, 2009b), Daulton et al. (2010) attempted to replicate that discovery at two well-known archaeological sites, Murray Springs, Arizona, and Arlington Canyon, California. Daulton et al. (2010) found no YDB NDs and concluded that their findings cast doubt on the presence of YDB NDs, although they pointed out that YDB NDs might "occur inhomogeneously and only in some of the YD-boundary carbons and hence are not observed in our study" (p. 16046). Daulton et al. (2010) also noted that other minerals, including nanocrystalline copper and copper oxide, could be misidentified as several of the proposed diamond polytypes, because of crystallographic similarities between copper and diamond.

Later, an independent YDB study by Tian et al. (2011) confirmed the discovery of cubic YDB NDs at Lommel, Belgium, in the charcoal-rich YDB layer in the upper part of a layer that is known regionally as the Usselo Horizon. The intersection between the Usselo layer and regional overlying cover sands has been long recognized as representing the onset of the YD climate change (Van Geel et al. 1989). At Lommel, cubic NDs were embedded in carbon particles but with no other ND polytypes, and no NDs were observed above or below the YDB layer. As with previous studies, the authors did not examine bulk sediment for NDs. Tian et al. (2011) concluded that the NDs alone did not represent indisputable evidence for a cosmic impact, but they did not exclude one.

Israde-Alcántara et al. (2012b) used multiple analytical techniques to demonstrate that the YDB NDs from Lake Cuitzeo, Mexico, are cubic NDs, n-diamonds, i-carbon, and lonsdaleite-like crystals. Israde-Alcántara et al. (2012b) also identified several problems and limitations of the study by Daulton et al. (2010), who reported an absence of YDB NDs in carbon spherules at Murray Springs and Arlington Canyon. First, Daulton et al. (2010) searched for and failed to find NDs within carbon spherules at Murray Springs, but neither Firestone et al. (2007) nor Kennett et al. (2009a) reported finding carbon spherules at that site, making the related absence of NDs unsurprising. Our investigations showed that carbon spherules are most common in regions having conifer trees at 12,800 cal BP, not in scrubby grasslands, as existed at Murray Springs at that time (Haynes and Huckell 2007). Second, at both sites Daulton et al. (2010) searched for NDs

in charcoal, which has never been reported by any workers to contain NDs. Third, Daulton et al. (2010) did not examine bulk sediment, the only source of NDs at Murray Springs reported by Kennett et al. (2009a).

Kennett et al. (2009b) reported NDs in carbon spherules at Arlington Canyon, California; Daulton et al. (2010) found no NDs there either, but there was a major flaw in their sample acquisition. The same coauthors of Daulton et al. (2010) claimed, in Pinter et al. (2011, p. 254), to have acquired their samples from a location "identical or closely proximal to the location" examined by Kennett et al. (2009a). Contradicting that statement, Wittke et al. (2013) noted that the Universal Transverse Mercator coordinates of their sampling sites show conclusively that their purported continuous sequence was actually collected as four separate discontinuous sections, separated by up to 7000 m horizontally from the sampling location of Kennett et al. (2009a, 2009b). Therefore, Scott et al. (2010) did not sample the YDB at the location studied by Kennett et al. (2009a) and did not acquire a dated, continuous profile across the YDB at any Arlington Canyon location. These mislocated sediment samples collected by Scott et al. (2010) were subsequently used in several different studies by the same group of authors (Daulton et al. 2010; Scott et al. 2010; Pinter et al. 2011). Their incorrect stratigraphic locations apply to all those investigations, explaining their inability to detect YDB NDs, cosmic-impact spherules, and ND-rich carbon spherules at Arlington Canyon.

Daulton (2012) also questioned the identification of lonsdaleite (hexagonal diamond), suggesting that some particles exhibited in Kennett et al. (2009b) appear to be graphene-graphane aggregates. Van Hoesel et al. (2012), Madden et al. (2012), and Bement et al. (2014) also reported finding graphene-graphane clusters with diffraction patterns similar to those of lonsdaleite. Boslough et al. (2012) suggested that some of the reported lonsdaleite from Lake Cuitzeo might instead be other minerals. We discuss these points below in "Identification of Lonsdaleite-Like Crystals."

Daulton (2012) and Boslough et al. (2012) questioned whether YDB NDs are robust cosmic-impact markers. However, cubic NDs are widely accepted to have formed during the K-Pg impact event and were not found in sediment before or after the event (Carlisle and Braman 1991; Gilmour et al. 1992; Hough et al. 1997, 1999). Those NDs are found at six coeval sites across North America: two in Colorado and one each in Mexico, Montana, and Al-

berta, Canada. The K-Pg NDs were reported to range in size from 1 nm to 30 μm, whereas YDB NDs are smaller, spanning a narrower range of ≈1 to ≈2.9 μm, perhaps because that older impact was larger and more energetic than the YDB event.

Van Hoesel et al. (2012) observed cubic NDs within particles of glass-like carbon at the Geldrop-Aalsterhut site in the Netherlands. The NDs were found in a few-centimeter-thick, charcoal-rich interval at the upper boundary of the Usselo layer, the top of which is widely accepted as representing the onset of the YD cooling episode (Van Geel et al. 1989). They reported NDs only in glass-like carbon in the bottom 1 cm of that interval and did not examine bulk sediment for the presence of NDs.

Recently, Bement et al. (2014) discovered an abundance peak in YDB n-diamonds (190 ppm) at Bull Creek, Oklahoma, independently confirming the discovery there of YDB NDs (100 ppb) by Kennett et al. (2009a). They did not observe cubic NDs, as Kennett et al. (2009a) did, and neither group observed lonsdaleite at Bull Creek. In addition, Bement et al. (2014) observed an ND abundance peak of similar amplitude to their YDB peak in two contiguous samples of late Holocene surface sediments (0–10 and 10–20 cm below surface). They suggested that this younger ND peak may have been produced by a nearby cosmic-impact event within the past several thousand years. This discovery may correlate with that of Courty et al. (2008), who discovered melt-glass and spherules at widely distributed sites in Syria, Spain, and Peru, localities separated by up to 13,000 km, as evidence for a ≈4000-yr-old Northern Hemispheric impact event. Bement et al. (2014) concluded from sedimentological evidence that the peak ND accumulations in the YDB and younger strata did not result from changes in climate, deposition rates, lag deposits, or human site usage. Their results refute the hypothesis that the NDs simply resulted from cosmic influx that deposited them as a lag deposit at the YDB over an extended interval of time (Haynes et al. 2010; Pinter et al. 2011; Boslough et al. 2012). Instead, Bement et al. (2014) concluded the evidence is consistent only with cosmic-impact events.

In summary, abundant NDs within or near the YDB layer have been reported by four independent groups (Redmond and Tankersley 2011; Tian et al. 2011; van Hoesel et al. 2012; Bement et al. 2014). In addition, NDs have been reported independently in three conference presentations (at Indian Creek, MT, by Baker et al. 2008; at Newtonville, NJ, by Demitroff et al. 2009; and at Bull Creek, OK, by Madden et al. 2012). These investigations independently confirm the presence of an ND abundance peak in the YDB layer, which has also been shown to be associated with a diversity of other cosmic-impact proxies. Research continues into the specific origin of the various YDB ND polytypes and the presence of lonsdaleite.

Material and Methods

We now present a comprehensive summary of the chemical processing methods that we used to extract and isolate NDs from terrestrial bulk sediments and glacial ice. This is followed by details of the characterization, identification, and interpretation of YDB NDs. The protocol here supersedes previous published versions for extracting YDB NDs (Kennett et al. 2009a, 2009b; Kurbatov et al. 2010; Israde-Alcántara et al. 2012b). Further details are in appendix A.

Our protocol was adapted by one of us (S. S. Que Hee) from the extraction procedure developed by Huss and Lewis (1995), who used it to isolate presolar NDs from meteorites. We found that the maximum yield of all types of NDs occurred after the ammonium hydroxide extraction step and that subsequent oxidation with perchloric acid destroyed many crystals of n-diamonds and i-carbon and, possibly, some of the lonsdaleite-like crystals. This was an advantage when analyzing cubic NDs but a major disadvantage for the other allotropes, which were no longer present. Although the extraction process remains difficult, exacting, and labor-intensive, we have successfully extracted NDs from hundreds of samples in or adjacent to the YDB layer on three continents and in the Greenland Ice Sheet, along with samples from the K-Pg impact, Sudbury Crater, and the Tunguska airburst. Six independent groups have successfully used this protocol or a version of it (Baker et al. 2008; Demitroff et al. 2009; Redmond and Tankersley 2011; Tian et al. 2011; van Hoesel et al. 2012; Bement et al. 2014).

Preparing Sediment and Ice. From each sedimentary sample collected, 500–1000 g of thoroughly mixed dry bulk sediment was processed through a clean, ultrasonicated <38-μm screen to concentrate the fine, ND-bearing fraction. A minimum of 20–150 g of the <38-μm fraction was used for extraction of NDs, whereas the >38-μm-size fraction was not used. Water was removed from bulk ice core samples by freeze-drying or by melting and evaporation before chemical processing. This method extracts unattached NDs within the sediment as well as any NDs that may be contained inside any melt-glass or small mineral aggregates. Great care was taken to eliminate contamination by industrial cubic NDs, and any such contamination is highly un-

likely, as indicated by the fact that NDs always peak in the same layer that contains other markers. Peaks of similar magnitude have never been found outside the YDB layers.

Materials and Equipment. All solutions were prepared with corresponding TraceMetal or Electronics-grade chemicals and concentrated acids or bases. A detailed list of standard instrumentation and equipment appears in appendix A.

Extraction and Purification. As many operations as possible were performed at room temperature, because temperatures above 200°C can cause noncubic types of NDs to gradually convert to other forms of carbon, such as graphite. Also, adequate rinsing and centrifugation are crucial for successful purification of the ND-rich residues.

The YDB NDs contain surface carboxyl groups (–COOH) formed in situ either during ND formation or during diagenesis while buried for 12,800 yr. These carboxyl groups are a key part of the extraction process, because they allow the NDs to go into suspension in basic solution, thus separating from the non-ND minerals. However, these carboxyl groups are also subject to decarboxylation under strongly acidic conditions and/or at elevated temperatures. Therefore, it is vitally important to extract any NDs into room-temperature basic solution (pH > 7) while they still contain the maximum density of carboxyl groups on their surfaces. After the samples were pulverized and massed, therefore, the first chemical step was extraction of NDs, using room-temperature 0.1 M NaOH. Once NDs were separated from the remaining sediment, they were consolidated in solution acidified to a pH of <2 with 9 M HCl.

Next, acidic dichromate oxidation ($K_2Cr_2O_7$ and H_2SO_4) was used to remove the remaining intractable organic components that might adhere to NDs. Following dichromate oxidation, samples were diluted with deionized water to lower solution density and were centrifuged. Supernatants were discarded, and residues were rinsed repeatedly with 0.1 M HCl. Some YDB residues were visible, but most were detectable only by light microscope. For non-YDB samples, often there were no residues visible with a light microscope.

At this point, most non-ND minerals were either left behind during basic extraction or oxidized by the acidic dichromate. Any remaining silicates were digested with 10 M HF/1 M HCl, and after rinsing, samples were treated with 9 M HCl to destroy fluorides. If necessary, the acidic dichromate and hydrofluoric acid steps were repeated. Finally, the samples were dried and weighed. The typical result was a very small amount of whitish-gray res-

idue that contained amorphous carbon and, if present, an assemblage of several types of NDs (cubic, n-diamonds, i-carbon, and lonsdaleite-like crystals). This was the last step performed if we chose to examine all types of NDs.

If we chose to investigate only the cubic NDs, an additional step was added to destroy the n-diamonds, i-carbon, and possibly lonsdaleite, thus making it easier to identify the cubic NDs. To accomplish this, we added concentrated perchloric acid ($HClO_4$, 70%), heated the mixture, and then allowed the perchloric acid to evaporate to dryness. After that, samples were rinsed several times with 0.1 M HCl and centrifuged. Once dried, the extracted ND residues were ready for further analysis. The acid extraction process commonly yielded very little residue that was nearly invisible to the naked eye inside the centrifuge tubes and often was detectable only by light microscope. For non-YDB samples, there were typically no residues visible even with a light microscope.

Early Developmental Studies. To test this protocol at the HF step, we used synthetic cubic NDs from PlasmaChem (PL-D-G-1g; avg. cluster size 4 nm; NDs usually ≤2 nm) at a concentration corresponding to 1000 ppm in 10 g of sediment. When the nitric acid was substituted for HCl, the HF/HNO_3 digestion step allowed recovery of 70%–80% by weight. The soluble phase contained 20%–30% of NDs by weight, and HCl acid-washing conditions resulted in quantitative recoveries in the solid residue at each such step. The recovery of spiked cubics up to the perchloric acid step varied between 70% and 80% in these preliminary experiments. The major step responsible for the variation was the flocculation step.

To determine the efficacy of the perchloric acid extraction step, we conducted several experiments. When 10 mg of synthetic cubic NDs was subjected to the perchloric acid processing step, 81% ± 5% was recovered by weight as unaltered cubic NDs. Transmission electron microscopy (TEM) confirmed the presence or absence of NDs in all these experiments, which confirmed that extraction of NDs with this protocol has a high success rate.

NDs from Carbon Spherules and Amorphous Carbon. The NDs were not extracted from carbon spherules; instead, the spherules were crushed to fine fragments and placed on a TEM grid, as described in detail in appendix A. Tian et al. (2011) and van Hoesel et al. (2012) reported YDB NDs in flakes of amorphous carbon or glass-like carbon, and our general protocol for carbon spherules also applies to NDs within these other forms of carbon.

Preparation of TEM Grids for Analyzing NDs. Cur-

rently, we use 200- to 400-mesh TEM grids of gold or molybdenum with ultrathin carbon film (≈3 nm thick) over holey carbon. It is important to note that because ultrathin films are approximately as thick as the NDs and other nanoparticles, they have the least effect on energy dispersive X-ray spectrometry (EDS) and other measurements, making their use essential for obtaining the best analyses. We avoided films that have large open holes (holey carbon) because the NDs are much smaller than the holes.

Some earlier ND work (Kennett et al. 2009*a*, 2009*b*; Kurbatov et al. 2010) was conducted on copper grids, which were discontinued because of the similarity between the spacings of crystallographic planes (d-spacings) of copper and some NDs (Daulton et al. 2010). Those early samples on copper grids were subsequently reanalyzed on gold or molybdenum grids and with additional analytical techniques, such as EDS and energy-filtered TEM (EFTEM) that can differentiate carbon from copper particles. The results confirmed that the use of copper grids, although suboptimal, did not lead to the misidentification of YDB NDs. In addition, although silicon films are preferable to carbon films for investigating carbon objects, we have discontinued their use because they are less stable under a high-voltage electron beam.

To prepare a TEM grid, we first placed NDs into suspension by pipetting just 1 or 2 drops of ammonium hydroxide (NH_4OH), ethyl alcohol, or deionized water into the vial and stirring the ND-rich mixture. Then we pipetted the drop onto the grid and dried it. For further details of preparing grids, see appendix A.

Experimental Methods: Electron Microscopy and Spectroscopy. Sample residues were examined with high-resolution TEM (HRTEM), scanning TEM (STEM), electron energy-loss spectroscopy (EELS), selected-area electron diffraction (SAD), and EDS. To accomplish that, we used an FEI 300-kV field emission gun Titan equipped with a Super Twin objective lens, a spherical-aberration-image corrector, an EDAX energy-dispersive spectrometer, a high-angle annular dark field (HAADF) detector, and a Tridiem Gatan imaging filter. For all of the experiments, the instrument was operated at 300 kV. The TEM detectors were calibrated for accuracy with commercial cubic diamond and gold standards (Ted Pella #646). Fast Fourier Transform (FFT) analyses of the HRTEM images and the analyses of the EELS data were performed with Gatan Digital Micrograph. Occasionally, JEOL 1200EX II and JEOL TEM 1210 transmission electron microscopes were operated at 80 kV to acquire images

with higher contrast and to investigate nanoparticles that vaporized at temperatures generated by the higher voltages of the Titan.

Difficulties in Identifying NDs. The extraction process detailed in this contribution yields a residue that contains amorphous carbon, resistant minerals, and NDs, when present, but there are technical difficulties in fully characterizing this material. For example, the protocol does not remove minor amounts of non-ND crystals, including quartz, rutile, and zircon. Typically, NDs represent <50% of the residue, and the remaining non-ND residue can mask the NDs, thus making them difficult to identify. In addition, there are inherent difficulties and uncertainties in correctly identifying tiny crystals <2 nm in diameter. Furthermore, multiple ND polytypes are often intermixed, making differentiation of individual polytypes difficult.

Quantification of NDs. Accurate quantification of ND abundances in a sample is difficult, because the volume of NDs present is typically minuscule and the NDs are difficult to isolate from amorphous carbon. We addressed this problem by adapting methods used by various researchers to semiquantify abundances of other kinds of particles, such as aciniform carbon (a form of soot), charcoal, foraminiferal species, and various plant microfossils. We developed an 11-point scale (0% to 100%) for estimating the abundances of NDs at parts-per-billion to parts-per-million levels in both the extracted residues and carbon spherules (see "Quantification of NDs" in app. A; fig. A1; app. C). The abundance values presented here supersede previously published values.

Results and Discussion

Regional Setting. The YDB ejecta field contains a variable assemblage of cosmic-impact markers, including NDs, cosmic-impact spherules, carbon spherules, and high-temperature melt-glass. The field spans an area of ≈50 million km^2 across four continents, with no known limits (Wittke et al. 2013). For this study, we investigated YDB NDs at 22 sites in 10 countries on three continents, and independent researchers conducted six studies, for a total of 24 sites (fig. 1). Thirteen sites are in the United States, two in Canada, two in the Netherlands, and one each in the Greenland Ice Sheet (Denmark), Belgium, Germany, Mexico, Spain, Syria, and the United Kingdom. These 24 sites occur across a remarkably diverse range of geologic settings, including polar ice, glacial till, mountain lakes, caves, coastal canyons, desert dry washes,

and alluvial terraces, with altitudes varying from near sea level to >1800 m. This wide diversity indicates that geologic setting has no effect on the presence of YDB NDs, as also concluded by Bement et al. (2014). Details on site setting, geological information, and dating are in tables D2, D3. More details for most sites are in Bunch et al. (2012) and Wittke et al. (2013).

Dating and Age-Depth Models. We present new radiocarbon dates for three sites (Lake Cuitzeo, Mexico; Lingen, Germany; and Santa Maira, Spain), and we have generated new age-depth models for Arlington Canyon (fig. B1) and Lake Cuitzeo (figs. B2, B3). We present ND data for 15 new sites, for which site details, stratigraphic information, and dating are provided in appendix B and tables D2, D3. Of the 24 sites investigated, 18 (75%) have either direct dates or age-depth models at sufficient chronological resolution to confirm correlation with the YDB. Three others have been indirectly dated via lithologic and isotopic stratigraphy, archaeological context, and age-depth modeling, and the remaining three sites lack dates directly from the YDB but have consistent extrapolated ages based on dated materials from near the boundary layer.

The dates for a few of these sites have been challenged. For example, Blaauw et al. (2012) questioned the age-depth model for the Lake Cuitzeo sediment core in Israde-Alcántara et al. (2012*b*) and proposed that the YDB layer is up to 2000 yr older than the modeled age. Israde-Alcántara et al. (2012*a*) countered that the modeled age is the only one consistent with palynological and climatological records from this sequence and several sites located in Central and South America. To further test the age model, we acquired a new accelerator mass spectrometry ^{14}C date (NOSAMS-71325: 10,550 ± 35 RCYBP, 12,897 ± 187 cal BP) on organic sedimentary carbon collected above the YDB layer in a nearby exposed shoreline sediment sequence, lithologically correlated with the lake core. This helps constrain the age of the ND-rich layer and demonstrates that the model previously published in Israde-Alcántara et al. (2012*b*) is correct (table D3; figs. B2, B3).

Boslough et al. (2012) questioned the age determination for the YDB at the Gainey, Michigan, site, on the basis of a modern date acquired for a YDB carbon spherule. That date replicated a modern date previously reported for the same stratum of the Gainey sequence (Firestone 2009). Also, Ives and Froese (2013) questioned the inferred YDB age for carbon spherules at the Chobot site in Canada, also on the basis of a young radiocarbon date from Firestone (2009). Nevertheless, the archaeological context argues against a modern age for these near-surface layers. At both the Gainey and Chobot sites, the inferred YDB layers contain glassy and magnetic cosmic-impact spherules, as well as carbon spherules, each filled with millions of NDs (see "TEM, SAD, and Scanning Electron Microscopy of NDs in Carbon Spherules" below). This impact evidence is associated with large numbers of temporally diagnostic, Clovis-era artifacts that are found near the surface but date within a range of ≈13,250–12,800 cal BP (Waters and Stafford 2007). Furthermore, the span of an OSL date (12,360 ± 1230 cal BP) for the same Gainey layer includes the onset of the YD at ≈12,800 cal BP and is not modern in age. Thus, on the basis of available evidence, these young radiocarbon dates do not accurately reflect the age of the inferred YDB layers at these sites.

Firestone (2009) presented several possibilities to explain these age discrepancies, and the most likely is the effects of bioturbation. At some sites, we observed distinctive root casts, formed from large taproots of trees that penetrated the YDB layer after the impact event occurred. After those roots decayed or burned, the resulting cavity filled with sediment containing younger charcoal and carbon spherules that mixed with the older carbon material. Because this is a common occurrence where the YDB is shallow, radiocarbon dating is unreliable for such sites and OSL dating is preferred (Bunch et al. 2012), as indicated by the older OSL date for the Gainey site. No matter the cause, the ages of these two sites remain poorly constrained. Nevertheless, 18 of the 24 sites with the same YDB markers are well dated, suggesting that the YDB layer is correctly identified at Gainey and Chobot (table D3).

Later, van Hoesel et al. (2012, p. 7652) suggested that NDs in the Netherlands at the Aalsterhut site are "two centuries younger than the diamonds reported by Kennett et al." (2009*b*) and therefore are from an unrelated event. They concluded this on the basis of an apparent age discrepancy between the mean age of the ND-rich layer at their site and mean age of the Arlington Canyon site in California. However, they overlooked the fact that the date for the Aalsterhut site fully overlaps those for many other YDB sites, including Murray Springs. To test their hypothesis, we performed Bayesian analysis (Bronk Ramsey 2009) and χ^2 testing (Ward and Wilson 1978) on the Arlington Canyon radiocarbon dates. Both methods indicate that the Arlington Canyon radiocarbon dates have nonnormal distribution and thus are unsuitable for averaging (fig. B1). Bayesian analysis is particularly useful in detecting outlier dates (nonnormal distribution),
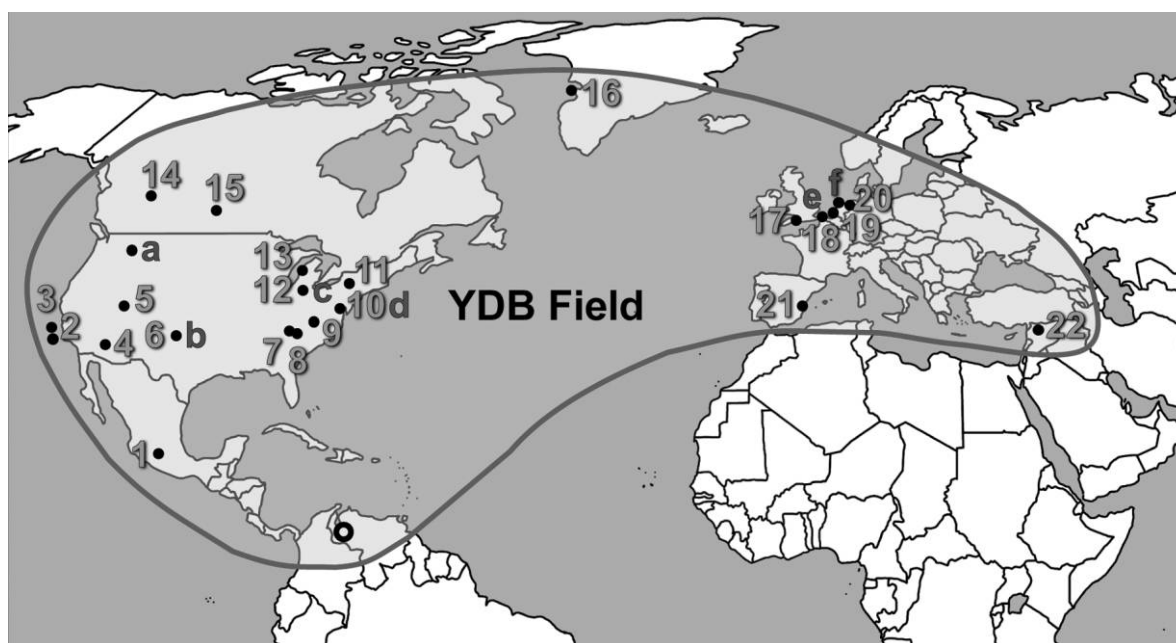
Figure 1. Map showing 24 sites containing Younger Dryas Boundary (YDB) nanodiamonds. The solid line defines the current known limits of the YDB field of cosmic-impact proxies, spanning 50 million km² (Wittke et al. 2013), including the study of Mahaney et al. (2010) in Venezuela (open circle). Numbered sites are from this study: (1) Lake Cuitzeo, Mexico (Israde-Alcántara et al. 2012*b*); (2) Daisy Cave, California; (3) Arlington Canyon, California (Kennett et al. 2009*b*); (4) Murray Springs, Arizona (Kennett et al. 2009*a*); (5) Lindenmeier, Colorado; (6) Bull Creek, Oklahoma (Kennett et al. 2009*a*); (7) Blackville, South Carolina; (8) Topper, South Carolina (Kennett et al. 2009*a*); (9) Kimbel Bay, North Carolina; (10) Newtonville, New Jersey; (11) Melrose, Pennsylvania; (12) Sheriden Cave, Ohio; (13) Gainey, Michigan (Kennett et al. 2009*a*); (14) Chobot site, Alberta, Canada (Kennett et al. 2009*a*); (15) Lake Hind, Manitoba, Canada (Kennett et al. 2009*a*); (16) Kangerlussuaq, Greenland (Kurbatov et al. 2010); (17) Watcombe Bottom, Isle of Wight, United Kingdom; (18) Lommel, Belgium; (19) Ommen, Belgium; (20) Lingen, Germany; (21) Santa Maira, Spain; (22) Abu Hureyra, Syria. In addition, independent researchers have reported NDs at six sites, indicated by letters, four of which are in common: (a) Indian Creek, Montana (Baker et al. 2008); (b) Bull Creek, Oklahoma (Madden et al. 2012; Bement et al. 2014); (c) Sheriden Cave, Ohio (Redmond and Tankersley 2011); (d) Newtonville, New Jersey (Demitroff et al. 2009); (e) Lommel, Belgium (Tian et al. 2011); (f) Aalsterhut, Netherlands (van Hoesel et al. 2012). A color version of this figure is available online.

including those that result from the old-wood effect, in which the date for charcoal or wood from a long-lived tree can lead to the erroneous conclusion that the stratum in which the charcoal was found is much older. Bayesian analysis rejected 14 of 16 Arlington Canyon dates as being outliers, consistent with the observation that local tree species have life spans of up to 1300 yr (see "Arlington Canyon, California" in app. B). After adjusting for the old-wood effect, OxCal modeled the YDB age for Arlington Canyon as 12,748 ± 46 cal BP (OxCal, ver. 4.2.3, IntCal-13; Bronk Ramsey 2009). This is statistically identical to the modeled YDB date for Aalsterhut of 12,746 ± 12 cal BP (10,870 ± 15 RCYBP; van Hoesel et al. 2012). These results contradict the hypothesis that the ND-rich layer at Aalsterhut is 200 yr younger than the ND-rich YDB layer at Arlington Canyon. Furthermore, van

Hoesel et al. based their 200-yr difference on the mean ages of the two sites, but the standard deviation must be considered, and using only mean ages is inappropriate. We conclude that van Hoesel et al. (2012) discovered the YDB layer at Aalsterhut. Bayesian analysis shows that the ages of all 18 well-dated YDB sites fall within 1 standard deviation of the YDB layer at 12,800 ± 150 cal BP, including Aalsterhut and Arlington Canyon (table D3). None of those 18 sites is 200 yr older than Aalsterhut.

Van Hoesel et al. (2014) also questioned whether the YDB proxies are synchronous with the onset of the YD climatic episode, which is widely accepted to have occurred abruptly. For example, in the NGRIP ice core, Steffensen et al. (2008) found that the YD onset occurred within a span of ≈1.5 yr, and Brauer et al. (2008) reported a similar narrow span of ≈1 yr in varved European lake records. The

Greenland Ice Core Chronology 2005 (GICC05; Rasmussen et al. 2006) found the mean age of the YD onset to be 12,896 ± 138 before 2000 AD (b2k; 13,034–12,758), and the GISP2 ice model (Meese et al. 1997) placed it at 12,892 ± 260 b2k (13,152–12,632). The YDB ages for 20 of 24 sites (83%) in table D3 fall within the ice core age ranges for the onset of the YD climatic episode, suggesting a close relationship between the YDB and the YD onset. Most importantly, a major peak in impact-related platinum in the GISP2 ice core occurred precisely at the onset of the YD climatic episode (Petaev et al. 2013), strongly indicating that the YDB cosmic-impact event and the onset of the YD episode are synchronous.

The YDB hypothesis posits that only one impact occurred, producing coeval, above-background peaks in NDs, iridium (Firestone et al. 2007), platinum (Petaev et al. 2013), osmium (Wu et al. 2013), high-temperature melt-glass (1730° to >2200°C; Bunch et al. 2012), and high-temperature magnetic spherules (>1500°C; Wittke et al. 2013). Others have proposed various age models for deposition of the YDB proxies. The first counterexplanation is that YDB proxies resulted from multiple, unrelated, natural mechanisms that coincidentally occurred near 12,800 cal BP (Pinter et al. 2011; Boslough et al. 2012; van Hoesel et al. 2014). To investigate that, our group and others have measured marker abundances in several stratigraphic profiles that span as much as the past 30,000 yr. These proxies reached maximum abundances only in the YDB layer and are not known to peak individually or collectively anywhere else in that span, making the YDB highly unusual. In the second scenario, the YDB proxies were deposited over several centuries, resulting from multiple discrete cosmic-impact events. However, current understanding of impact dynamics cannot explain how such a scenario could occur over such a span. In the third scenario, the YDB proxies were deposited during a span of up to several decades. Such a situation could occur if the debris field of a fragmented comet or asteroid was oblique to or wider than Earth's diameter upon impact. In such a case, some objects would have encountered Earth at an oblique angle and could have assumed orbits that decayed over a few years to decades, producing multiple smaller impacts (Fawcett and Boslough 2002; Petaev et al. 2013). The fourth and most plausible scenario, the one most consistent with our data, is that only one hemispheric impact event occurred. This is supported by the platinum record in GISP2, which forms a single, brief, coherent abundance peak, the only one within the 280-yr interval investigated.

Abundance and Stratigraphic Distribution of NDs. Crystal morphologies vary from angular to rounded and from monocrystalline to twinned, and ND diameters average 3–4 nm (range: 1 nm–2.9 μm), with most measuring between 1 and 20 nm, a typical size for detonation-formed NDs (Wen et al. 2007). The quantification method discussed above was used to estimate abundances of NDs and revealed concentrations in carbon spherules of 10–3680 ppb (mean: 755 ppb) and in bulk sediment of 11–494 ppb (mean: 200 ppb). For carbon spherules, 111 of 153 samples investigated (73%) contained no detectable NDs, and for sediment, 57 of 87 (66%) samples had no evident NDs, comparable to the null results of Bement et al. (2014). Appendix A discusses quantification, figure 2 shows abundance peaks in NDs, and table D4 lists the stratigraphic abundances of NDs for 22 sites. Table D4 also lists abundances of cosmic-impact spherules and melt-glass for 16 sites; the other six sites have not yet been examined for those proxies. All sites exhibit sharp ND abundance peaks at the YDB, with very few NDs in the strata above and below (fig. 2). For some sites, the peaks are broader, with elevated abundances of NDs in several contiguous samples. These secondary peaks most likely result from bioturbation and wind-and-water action that redistributed the NDs upward and/or downward.

Identification and Taxonomy of YDB NDs

Overview. Unknown nanoparticles were investigated with multiple analytical techniques; a nanoparticle was conclusively identified as an ND if several basic properties were documented: first, the nanoparticle is composed only of carbon; second, it has a crystalline structure; and finally, the d-spacings match those of an ND polytype. Although it is unnecessary to use all of the analytical procedures described below for every particle, at a minimum, we used EDS to determine elemental composition and HRTEM, SAD, and/or FFT to determine crystalline structure for all nanoparticles imaged in this contribution. These analyses were strengthened by use of EELS and EFTEM to assist with determining elemental compositions and to investigate the interatomic bonding typical of carbon (sp^2 and/or sp^3).

Electron Microscopy (TEM, HRTEM, and STEM). The STEM mode (HAADF, dark field) was typically used to investigate candidate nanoparticles, but the quality of the images was often degraded by scattering of electrons by the amorphous residue and by contamination of the grid by vaporized carbon. The TEM and HRTEM modes (bright field) typi-
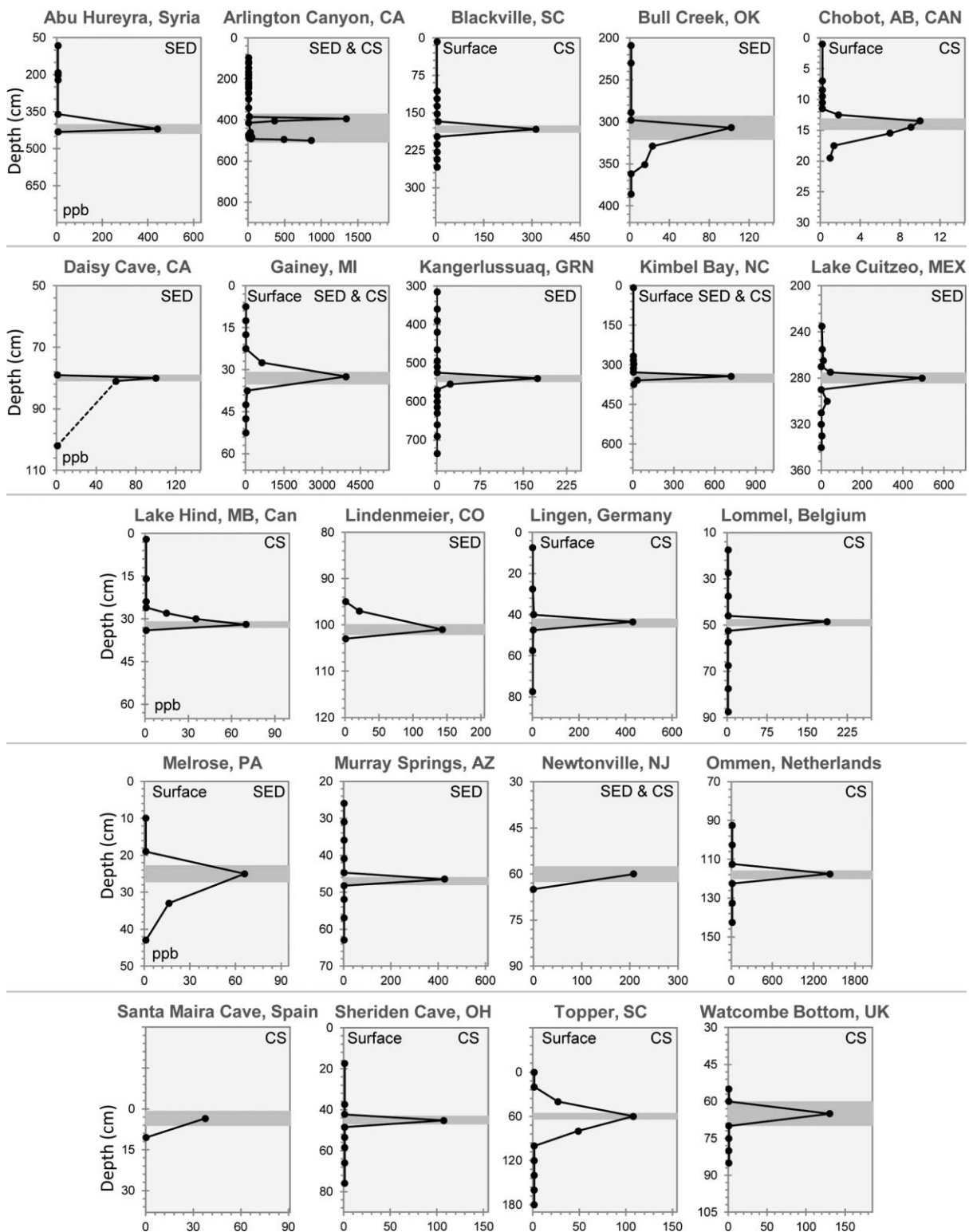
Figure 2. Abundances of nanodiamonds (NDs; ppb) for 22 Younger Dryas Boundary (YDB) stratigraphic sections plotted by depth (cm below surface). Most of the six independent studies did not quantify NDs at or near the YDB and are not represented here. Horizontal bands represent thicknesses of samples containing YDB proxies. Solid lines represent ND abundances (ppb), shown on the *X*-axis. ND abundances were estimated with an 11-point semiquantification scale of relative values ranging from 0% to 100% (see "Quantification of NDs"). CS = NDs extracted from

cally produced clearer images of NDs located in residue, thus strengthening analyses of crystallinity and lattice spacings.

Figure 3 illustrates the typical progression necessary to identify NDs. First, extracted material from Murray Springs and Lake Cuitzeo produced STEM images that show thousands of rounded-to-subrounded, nanosized particles (fig. 3*A* and 3*B*, respectively). At this point, it was unknown whether they were amorphous or crystalline. Next, an HRTEM image (fig. 3*C*) revealed the crystalline structure of NDs ("ND"), among a background of amorphous carbon and strand-like carbon ribbons ("CR") that are commonly present in the diamond-rich residue. Finally, an HRTEM image of a carbon nanocrystal (fig. 3*D*) displayed lattice spacings of 2.06 Å, consistent with (111) planes for cubic diamond (table D1), when viewed along the [110] zone axis. Additional testing typically was performed on these nanocrystals, as discussed below.

SAD and FFT of HRTEM. The SAD image from Murray Springs (fig. 4*A*) displays a ring pattern of collective d-spacings from multiple crystals, and in this case, all eight visible reflections match those of cubic NDs. Values for graphene and graphane are similar to those for six of those reflections, but the (400) and (551) reflections are not present in those other crystals (table D1). Their absence in SAD patterns for graphene and graphane makes those minerals easily detectable, thus eliminating the possibility of misidentification. By themselves, SAD patterns are insufficient to identify NDs, and so further investigations, such as those using HRTEM, FFT, EDS, and EELS, were performed on these nanoparticles to confirm that they are NDs and not some other mineral. The FFT of an HRTEM image of multiple nanocrystals (fig. 4*B*) shows three ring reflections that match the SAD pattern for cubic NDs. The FFT of an HRTEM image of a single nanocrystal (fig. 4*C*) displays (111)- and (220)-type spot reflections consistent with a single cubic diamond viewed along the [110] zone axis. Figures 5 and 6 show TEM, HRTEM, and SAD patterns for NDs found in bulk sediment and carbon spherules from sites on three continents. Results from 10 other sites are shown in figures C1–C6.

EDS. A STEM image from Lake Cuitzeo (fig. 7*A*) shows a nanoparticle field with the specific area of investigation boxed near the center. The SAD pattern of that boxed area (fig. 7*B*) exhibits diffraction rings characteristic of i-carbon. The EDS analysis of the boxed area (fig. 7*C*) indicated a carbon concentration of >98% as well as low amounts of oxygen and a weak signal from the gold grid, but no other elements. Because this analysis encompasses nanocrystals, the grid film (3-nm thick), and surrounding amorphous carbon, the elemental percentages for the nanoparticles are inexact but are dominantly carbon. When other mineral grains were encountered, e.g., quartz, rutile, and zircon, they were easily identifiable with EDS. Another STEM image (fig. 7*D*) shows a cluster of angular synthetic cubic NDs (97% pure 4-nm clusters from PlasmaChem) with no observable amorphous carbon; the box indicates the region being analyzed. An SAD pattern (fig. 7*E*) exhibits diffraction rings, indicating that the nanoparticles are cubic NDs, with no diffraction rings of other minerals. The EDS spectrum of the commercial diamonds in figure 7*F* shows >97% carbon, which closely matches the EDS of YDB NDs in figure 7*C*, with a similarly high abundance of carbon.

EELS. The EELS analyses were performed to determine whether selected nanoparticles are carbon and whether they display the correct atomic bonding for diamond. This is diagnostic for distinguishing cubic NDs and lonsdaleite-like crystals from other forms of carbon. The EELS technique is less useful for differentiating n-diamonds, i-carbon, graphite, and other carbon allotropes from each other, since these produce similar spectra. To differentiate the various carbon polytypes, it is also necessary to acquire SAD patterns and FFTs of HRTEM images.

The Murray Springs EELS spectrum, known as a core-loss spectrum (fig. 8*A*), displays the typical shape for cubic diamond (Peng et al. 2001). The σ^* edge is well above background, indicating that the nanoparticles are carbon. The small π^* edge is representative of lower-order sp^2 bonding, as found in graphite, graphene, graphane, and amorphous carbon. In this case, the peak most likely represents the carbon grid film and amorphous carbon in which the NDs are embedded. The two peaks at 300 and 310 eV with a trough between them represent the characteristic signature of cubic dia-

carbon spherules; SED = NDs from bulk sediment; "surface" indicates ground surface for eight sites; no NDs were observed in these surface layers. Abundances for NDs, carbon spherules, and cosmic-impact spherules are listed in table D4, available online. Data are from Kennett et al. (2009*a*, 2009*b*), Kurbatov et al. (2010), and Israde-Alcántara et al. (2012*b*). A color version of this figure is available online.
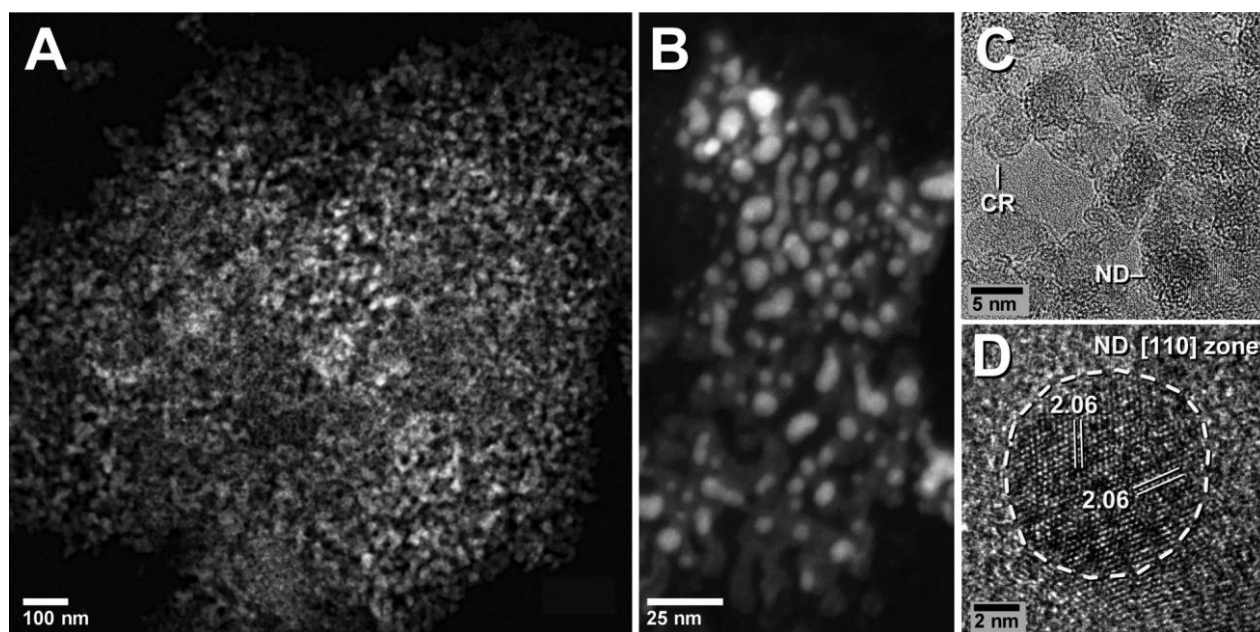
Figure 3. Three techniques for identifying candidate nanodiamonds (NDs). *A*, *B*, Scanning transmission electron microscopy images of clusters of NDs from Murray Springs, Arizona (Younger Dryas Boundary [YDB]: 426 ppb of NDs at 46.5 cm below surface [cmbs]; *A*), and Lake Cuitzeo, Mexico (YDB: 493 ppb at 280 cmbs; *B*). *C*, Bright-field high-resolution transmission electron microscopy (HRTEM) of ND-rich residue from Murray Springs. CR = carbon ribbon. *D*, HRTEM image of a rounded cubic ND at Lake Cuitzeo. Parallel lines represent {111}-type lattice planes (2.06-Å spacing), as viewed along the [110] zone axis. A color version of this figure is available online.

mond with sp^3 bonding. This pattern definitively eliminates the possibility that these nanocrystals are graphite, graphene, and graphane.

The EELS plot in figure 8*B* is of synthetic commercial cubic diamond (PlasmaChem) and closely resembles the YDB spectrum. Note that the π^* peak is absent in this case, because of the lack of embedding amorphous carbon matrix in the commercial diamonds. The Murray Springs EELS spectrum (fig. 8*C*) indicates a mix of mostly n-diamonds and i-carbon and is significantly different from the EELS spectrum for the synthetic cubic diamond. In this case, a π^* peak is present, indicating some sp^2 bonding, consistent with n-diamond, which is reported to contain approximately 5% sp^2 and 95% sp^3 bonding (Peng et al. 2001). The absence of a peak-and-trough pattern (arrows in fig. 8*A*, 8*B*) indicates that the nanoparticle is not a cubic ND. This spectrum is a close match for previously published spectra for n-diamond and i-carbon (curved lines above the spectra) but is a poor match for graphite, graphene, and amorphous carbon, which typically display π^* peaks with greater amplitude, indicating proportionately more sp^2 bonding. Thus, low-amplitude π^* peaks can be used to infer that a particle is likely a diamond polytype.

EFTEM. We used EFTEM in some cases as an

elemental mapping technique to investigate the spatial distribution of carbon and to examine its relative atomic bonding (sp^2 and sp^3), as was first used for YDB NDs by Tian et al. (2011). Figure 9*A*, from the YDB layer in Lake Cuitzeo, is called a "zero-loss" image, exhibiting various lighter nanocrystals embedded in the grayer amorphous carbon residue, itself superimposed on the darker amorphous carbon TEM grid film, marked "AC." This image is displayed in reverse contrast for clarity. Using HRTEM and FFT, we identified and labeled the larger nanocrystals by polytype; in this view, n-diamonds, i-carbon, and cubics have a ratio of 3 : 1 : 1. There is also one lonsdaleite-like crystal, with a relative abundance that is atypically high in this case. Next, we generated a "jump ratio" image (fig. 9*B*) by comparing postedge energies characteristic of carbon (σ^* edge) with background energies ($\approx$260 eV). The resulting map displays bonding differences for the larger particles, whose bright gray-to-white contrast indicates the presence of some amount of sp^3 bonding that is characteristic of NDs but not of graphite, graphene, and graphane. The black-colored areas (AC) represent the TEM grid film, composed of amorphous carbon with no sp^3 bonding.

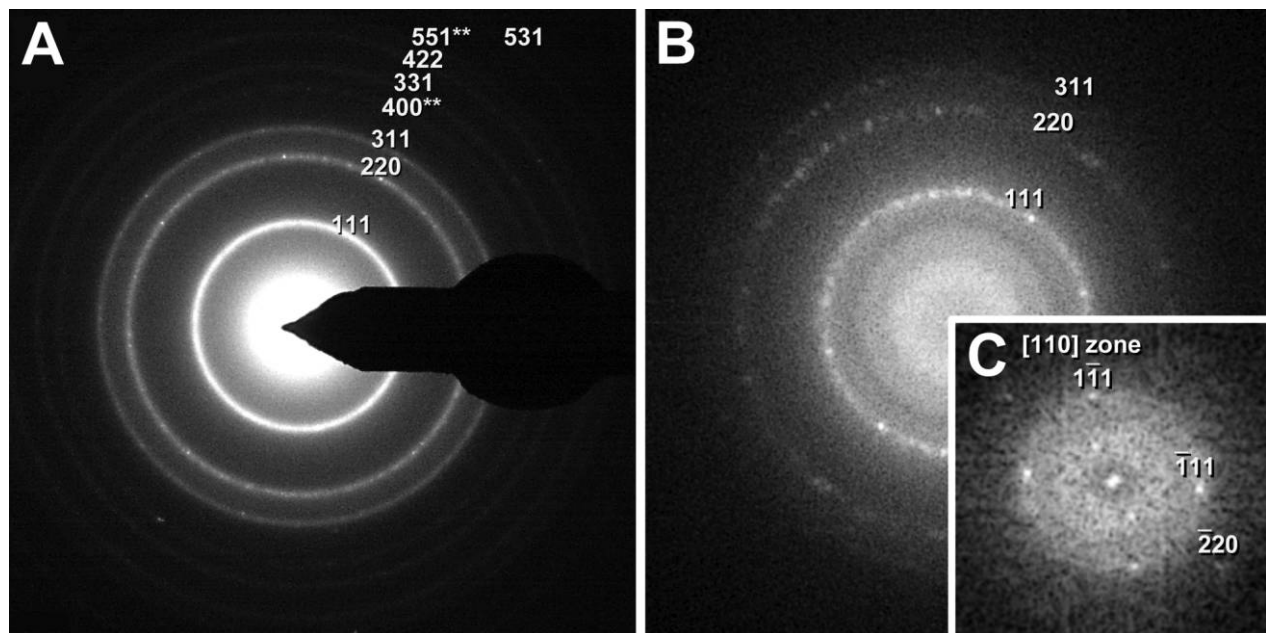The brighter areas between particles indicate the

Figure 4. Two techniques for identifying cubic nanodiamonds (NDs). *A*, Selected-area electron diffraction pattern of cubic NDs from Murray Springs, with d-spacings (Younger Dryas Boundary: 426 ppb at 46.5 cm below surface). *B*, Fast Fourier transform (FFT) of cubic NDs from Murray Springs; *C*, FFT of single cubic ND from Murray Springs, viewed along the [110] zone axis. A color version of this figure is available online.

presence of small, sub-nanometer nanoparticles displaying sp³ bonding, and this observation, along with the visible whitish-gray color of most residues, indicates that there is very little black, amorphous carbon present. Instead, the residue between NDs appears to consist of diamond-like nanocrystals arranged in short-range ordering that causes them to appear amorphous. It is possible that these are diamondoids, which are cage-like, ultrastable, saturated hydrocarbons (de Araujo et al. 2012), whose carbon-carbon lattice framework is largely identical to a portion of the cubic ND lattice. Diamondoids are found in hydrocarbon and coal deposits; they are nearly as hard as diamonds; each diamondoid typically includes from 10 to 30 carbon atoms; they are composed almost entirely of sp³-bonded carbon (de Araujo et al. 2012); and diamondoid powder can be visibly whitish to clear (Schoell and Carlson 1999). Diamondoids compare favorably to most of the crystals in the extracted residue, which also are dominantly carbon, have sp³ bonding, produce a diffuse SAD pattern because of their small size, and are optically clear to white. Because both n-diamonds and diamondoids have been found in petroleum deposits related to the K-Pg, one might speculate that something similar happened during the YDB impact, especially if an impact took place in deep, petroleum-rich offshore sediments.

More work is necessary to determine the nature and identity of these small nanoparticles, but they may be a clue to the YDB ND formation process.

The NDs in figure 9*B* typically are brighter around their edges but somewhat darker in their centers. This variability highlights a disadvantage of using EFTEM, which works best with thin layers of NDs and/or amorphous carbon residue. Because the fraction of electrons that undergo a single scattering event in a thick area is less than that in a thinner area, the jump ratio map shows a stronger EFTEM signal in the thin areas, even though both areas are equally populated by NDs.

Identification of n-Diamonds and i-Carbon. The YDB layer contains two diamond-like polytypes, n-diamonds and i-carbon, that were first synthesized in the laboratory (Wen et al. 2007 and references therein). Outside of the laboratory, face-centered cubic NDs (another name for n-diamonds) were first reported within carbon spherules from near-surface sediments of unknown age across northern Europe by Rösler et al. (2006). Later, both n-diamonds and i-carbon were found in the YDB layer (Kennett et al. 2009*a*) and the K-Pg layer (Bunch et al. 2008, 2009).

The YDB n-diamonds display the same d-spacings as cubic NDs, except for the added presence of so-called "forbidden" reflections evident in SAD
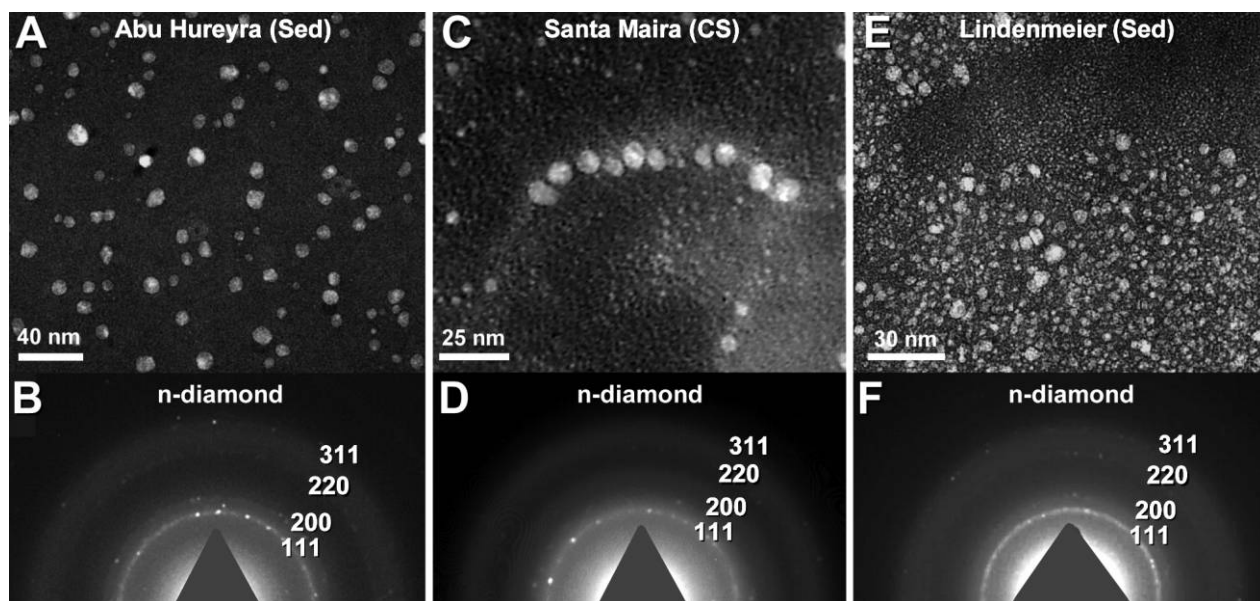
Figure 5.   Transmission electron microscopy images (in reverse contrast for clarity; *top*) and selected-area electron diffraction patterns (*bottom*) of nanodiamonds from three continents. *A*, *B*, n-Diamonds from sediment (Sed) at Abu Hureyra, Syria (Younger Dryas Boundary [YDB]: 443 ppb at 405 cm below surface [cmbs]). *C*, *D*, n-Diamonds in carbon spherules (CS) at Santa Maira Cave, Spain (YDB: 38 ppb at 3.5 cmbs). *E*, *F*, n-Diamonds from sediment at Lindenmeier, Colorado (YDB: 143 ppb at 101 cmbs). A color version of this figure is available online.

patterns and FFTs of HRTEM images (table D1). The lattice planes that produce these reflections are present in both cubic and n-diamonds, but as a result of destructive interference, the reflections are typically invisible in cubic NDs, hence the term "forbidden." These reflections may become visible in cubics for several reasons: first, because of double diffraction caused by the twinning; second, as a result of flaws caused by the occasional substitution of other elements for carbon atoms; and third, because of incomplete unit cells at the edge of the crystal. Thus, it is possible that n-diamonds are actually twinned cubic NDs.

A TEM image from Murray Springs (fig. 10*A*) exhibits more than 100 NDs that are tilted +30° from normal in the microscope. A second TEM image (fig. 10*B*) shows the same NDs, but tilted through a 45° arc to −15°. Note that corresponding objects appear similar in both images (e.g., particles 1–4), indicating that they all are rounded to subrounded and not planar. An SAD pattern of the same objects (fig. 10*C*) indicates that these are n-diamonds.

SAD, FFT, and HRTEM for n-Diamonds and i-Carbon.   An SAD pattern from Murray Springs (fig. 11*A*) displays seven lattice spacings of n-diamonds (table D1); EDS analyses confirmed these particles to be composed of carbon. The FFT of an HRTEM image (fig. 11*B*) shows five d-spacings of a single n-

diamond, and the HRTEM image of the same n-diamond (fig. 11*C*) shows three values representing two lattice planes, of which the 1.78-Å plane is a forbidden reflection in cubic NDs. The SAD pattern for Lake Cuitzeo material (fig. 11*D*) displays the first seven lattice spacings of i-carbon crystals. The FFT of the HRTEM image of a single i-carbon crystal (fig. 11*E*) shows three values representing two lattice planes, and the HRTEM image of the same i-carbon crystal (fig. 11*F*) shows three values representing two lattice planes, as viewed along the [001] zone axis. The EDS, EELS, and EFTEM analyses are not shown for these NDs but are similar to the analyses above for NDs.

Twinning in YDB NDs.   The YDB NDs larger than ≈2 nm are usually made up of two or more crystals that share a common lattice plane (the twin plane) and grow symmetrically in different orientations; twinned NDs were observed at all YDB sites. Twinning is also commonly observed in meteorites, cosmic-impact craters, and commercial NDs (Israde-Alcántara et al. 2012*b* and references therein). Twins can form in numerous configurations, including "star twins," as observed by Tian et al. (2011) in the YDB layer from Lommel. Figure 12*A* shows a multiply twinned ND from Kangerlussuaq, Greenland, composed of >20 individual crystals with lattice plane spacings and angles character-
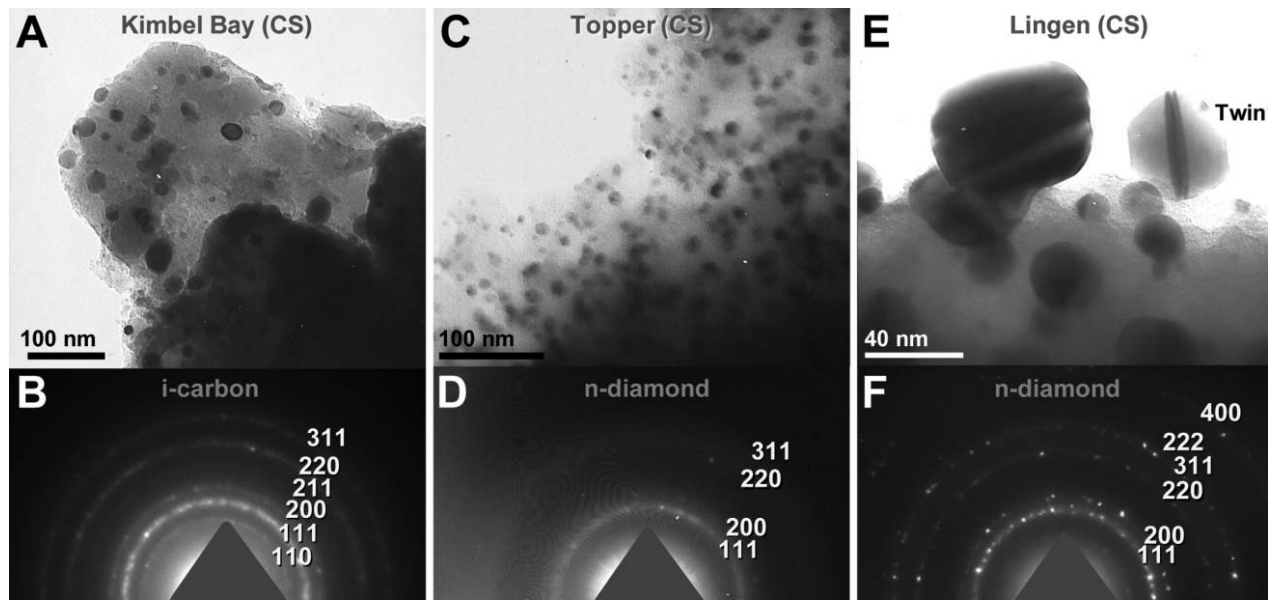
Figure 6. Transmission electron microscopy images (*top*) and selected-area electron diffraction patterns (*bottom*) used to identify nanodiamonds (NDs) in carbon spherules (CS). *A, B*, i-Carbon from Kimbel Bay, North Carolina (Younger Dryas Boundary [YDB]: 721 ppb at 351 cm below surface [cmbs]). *C, D*, n-Diamond from Topper, South Carolina (YDB: 108 ppb at 60 cmbs). *E, F*, n-Diamond from Lingen, Germany (YDB: 431 ppb at 43.5 cmbs); note twin ND at upper right. A color version of this figure is available online.

istic of n-diamond, as reported by Yang et al. (2008). Figure 12*B* is an FFT of the central crystal and displays eight lattice spacings that are consistent with n-diamonds and cubic NDs. Figure 12*C* is a "star-twin" n-diamond, so named because of its fivefold star-like symmetry. More twinned n-diamonds are shown in figure C6.

TEM, SAD, and Scanning Electron Microscopy of NDs in Carbon Spherules. Figure 13*A*, from Gainey, Michigan, is a TEM image of a carbon spherule fragment, showing embedded NDs as black dots within the amorphous matrix at the arrow. The EDS analyses indicate that these are carbon particles. Figure 13*B* is a photomicrograph of a typical YDB carbon spherule. Figure 13*C* is an SAD pattern, demonstrating that the particles are n-diamonds with a possible minor admixture of other NDs. Figure 13*D* is an HRTEM image from the Chobot site of a carbon spherule fragment containing NDs, such as the dark object marked by the arrow. This fragment was removed from inside a carbon spherule with a needle, demonstrating that some NDs form throughout the interior matrix of the spherules. The photomicrograph (fig. 13*E*) shows a carbon spherule with a hollow interior. Figure 13*F* is an SAD pattern demonstrating that these particles are n-diamonds. The NDs found in carbon spherules are indistinguishable from the

rounded NDs initially discovered by Rösler et al. (2006) and reported in Yang et al. (2008).

We investigated whether NDs always are distributed throughout the interior matrix of carbon spherules and glass-like carbon, the latter of which has been reported to contain NDs (van Hoesel et al. 2012). We used a focused ion beam to mill a piece of glass-like carbon extracted from the YDB layer at the M33 site, the rim of a Carolina bay in Myrtle Beach, South Carolina (for site details, see Firestone et al. 2007). The TEM analyses showed that diamonds were present only from the surface down to a depth of ≈ 0.75 μm and were not observed in the interior (fig. 14*A*). The surface layer was sharply demarcated and fused to the interior of the spherule. Figure 14*B* shows a chip of the glass-like carbon surface layer removed with a needle; it contains hundreds of densely packed NDs. Similarly, examination of carbon spherules from Watcombe Bottom, United Kingdom, suggested that some NDs were clustered in a thin layer on the outside of carbon spherules (fig. 14*C*). On the other hand, the carbon spherule fragment from the Chobot site (fig. 13*D*) displays NDs from deep within a spherule, and Rösler et al. (2006) reported NDs attached to the inner surfaces of vesicles in European carbon spherules. These results indicate that at least some NDs form only on surfaces of carbon spherules and
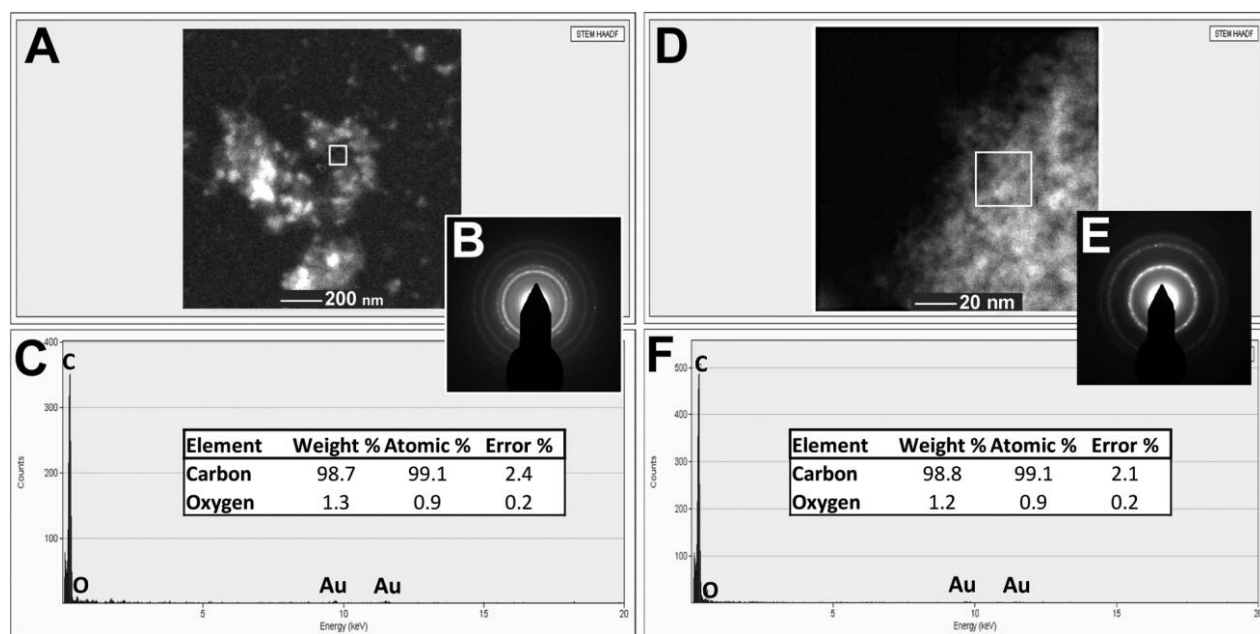
Figure 7. Scanning transmission electron microscopy (STEM) images (*A*, *D*), selected-area electron diffraction patterns (*B*, *E*), and energy-dispersive X-ray spectrometry plots (*C*, *F*) for elemental abundance of carbon: Younger Dryas Boundary nanodiamonds (NDs) from Lake Cuitzeo (493 ppb at 280 cm below surface; *A–C*) and synthetic NDs from PlasmaChem (*D–F*). Carbon in both is greater than ≈98%. HAADF = high-angle annular dark field. A color version of this figure is available online.

glass-like carbon, whereas others form throughout them. The reason for this difference is unclear, but finding NDs on spherule surfaces is consistent with one scenario, in which molten carbon spherules and glass-like carbon in an impact fireball were exposed briefly to anoxic conditions and high temperatures that caused NDs to form on their surface

layers, but not inside them, while preventing the carbon from incinerating.

Identification of Lonsdaleite-Like Crystals. Potential YDB lonsdaleite crystals have been identified and analyzed with HRTEM, FFT, SAD, and EDS (see Kennett et al. 2009*b*; Kurbatov et al. 2010; Israde-Alcántara et al. 2012*b*). On the basis of EDS
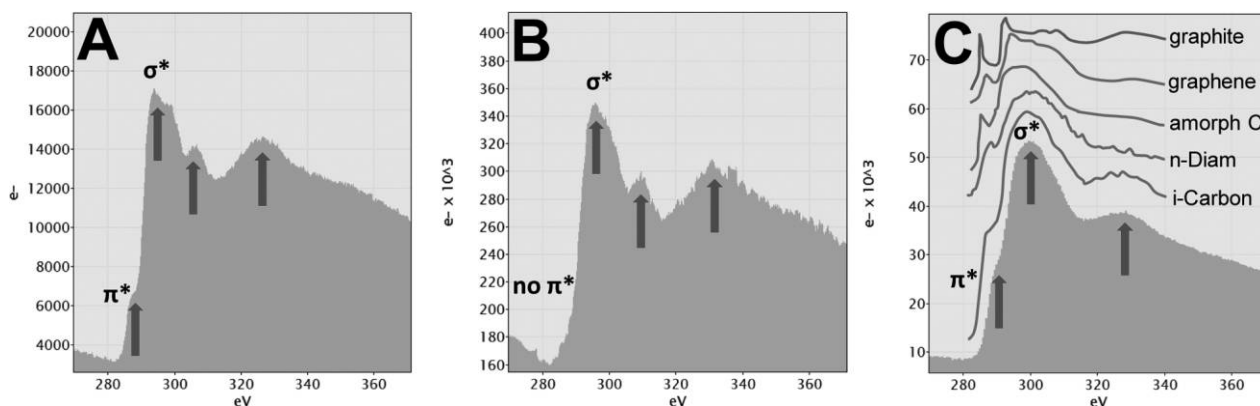

Figure 8. Electron energy-loss spectroscopy spectra for differentiating cubic nanodiamonds (NDs) from n-diamonds, i-carbon, and other forms of carbon. *A*, Younger Dryas Boundary (YDB) NDs from Murray Springs (426 ppb at 46.5 cm below surface). *B*, Synthetic cubic NDs. *C*, YDB n-diamonds from Murray Springs; solid lines represent spectra for graphite, amorphous carbon, n-diamond, and i-carbon from Berger et al. (1988); the graphene spectrum is from Daulton et al. (2010). A color version of this figure is available online.
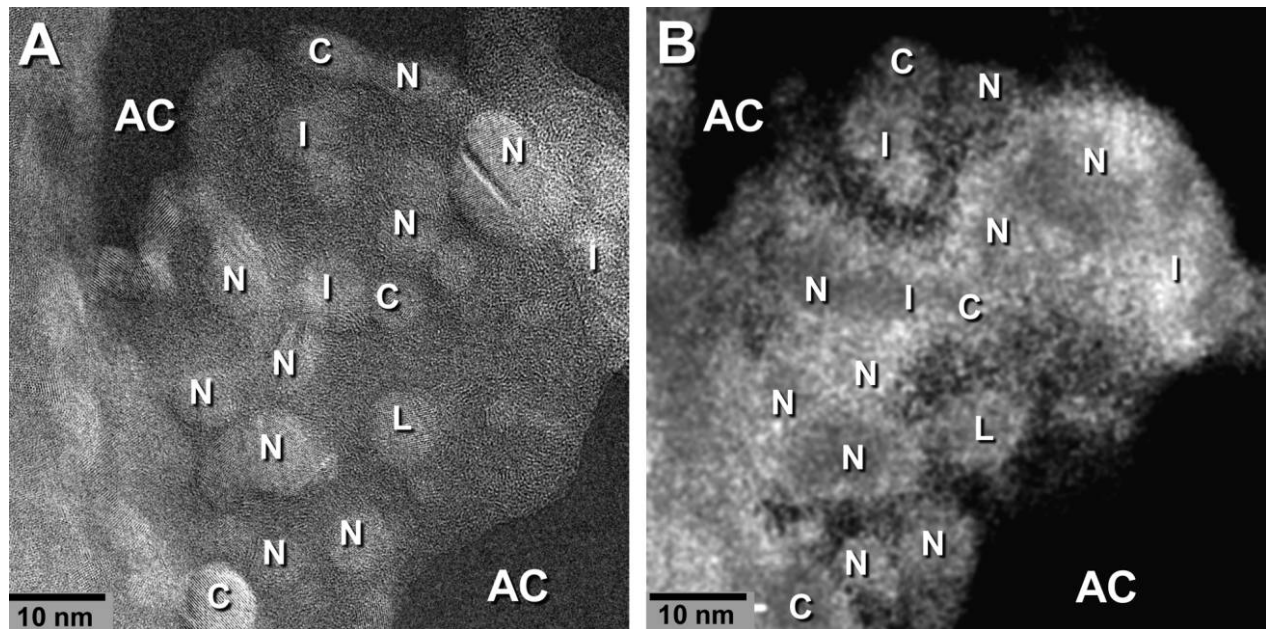
Figure 9. Energy-filtered transmission electron microscopy (EFTEM) for identifying carbon bonding in particles. *A*, Nanodiamonds (NDs) from Lake Cuitzeo (Younger Dryas Boundary: 493 ppb at 280 cm below surface) in a zero-loss EFTEM image (reverse contrast for clarity). *B*, Jump ratio map, exhibiting NDs with sp³ bonding in the lighter areas (reverse contrast for clarity). N = n-diamond; I = i-carbon; C = cubic diamond; L = lonsdaleite-like crystal; AC = amorphous carbon grid film. A color version of this figure is available online.

and EELS measurements, all the lonsdaleite-like crystals observed contain only carbon, with no other elements present but oxygen, eliminating the possibility that they are unidentified, noncarbon mineral. We have observed the crystals along three major zone axes ([0001], [01$\bar{1}$1], and [11$\bar{2}$1]), and all measured lattice planes are consistent with lonsdaleite and no other known carbon allotrope, including graphite, graphene, and graphane. Nevertheless, these crystals are too rare to allow definitive identification with all available analytical methods. Because many new, very hard forms of carbon have been discovered within the past few decades, these crystals may be some unidentified, diamond-like carbon allotrope. Therefore, we consider the identification of lonsdaleite to be provisional, pending further work. We include the evidence below for the benefit of other researchers.

Daulton (2012) questioned the identification of lonsdaleite in Kennett et al. (2009b), and we agree that the one cluster of nanoparticles in figure 2D–2F of the latter paper appears to consist of graphene-graphane aggregates, which mimic the d-spacings of lonsdaleite. We thank Daulton (2012) for pointing this out. He also questioned figure 2A–2C of Kennett et al. (2009b). Although the analyses were insufficient to conclusively identify the nanocrystal shown as lonsdaleite, we find no evidence to

eliminate it as a possibility, as discussed below in "Angular Lonsdaleite-Like Crystals."

Nearly all lonsdaleite observed in known impact craters is angular (Koeberl et al. 1997), and occasionally, YDB lonsdaleite-like crystals have been observed that are angular (Kennett et al. 2009b). However, in most cases, YDB NDs are rounded to subrounded in shape. The rounded lonsdaleite-like crystals may be due to modification by the extraction process, but this seems unlikely because acid-extracted n-diamonds are morphologically identical to nonacidized n-diamonds found in carbon spherules. Alternately, the rounded shapes may result from a different mode of formation. For example, subrounded to rounded commercial lonsdaleite has been produced by microplasma dissociation of ethanol vapor (Kumar et al. 2013), under conditions somewhat similar to those in an impact event, i.e., anoxic atmosphere and a carbon source. Below, we describe some analyses used to characterize the lonsdaleite-like crystals.

Angular Lonsdaleite-Like Crystals. A single YDB site, Arlington Canyon, California, contains flake-like lonsdaleite-like crystals (Kennett et al. 2009b), a shape similar to that of previously reported cubic NDs (Rösler et al. 2006) and plate-like lonsdaleite from known impact craters (Koeberl et al. 1997). A STEM image shows a tabular lonsdaleite-like crys-
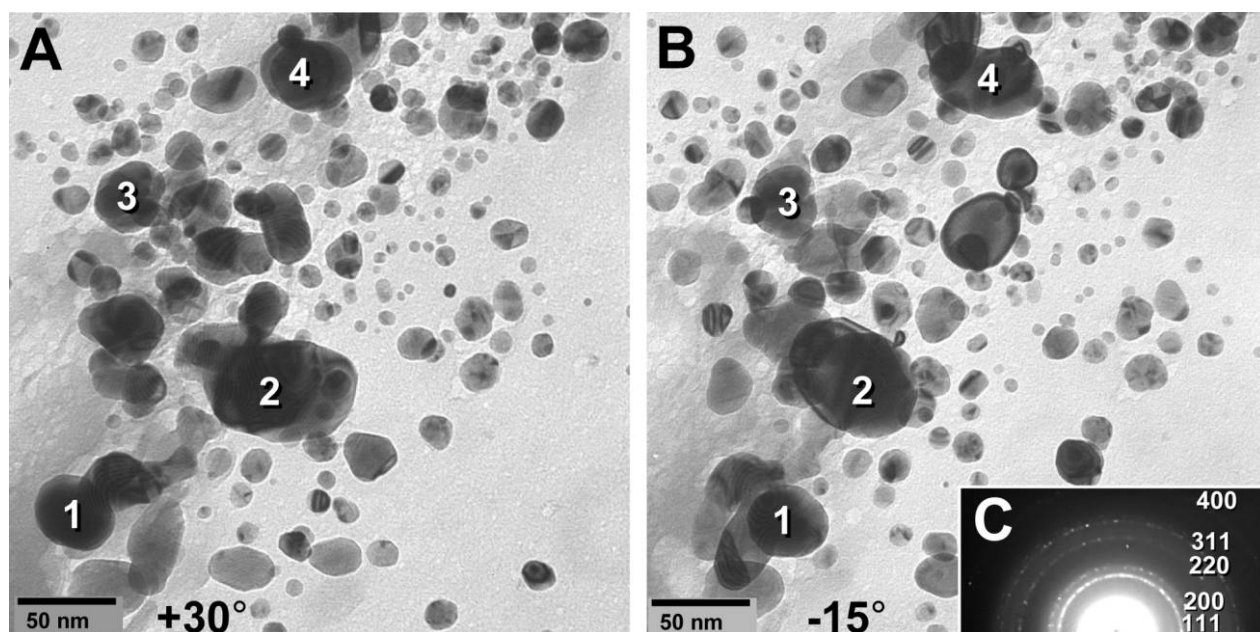
Figure 10. Tilted transmission electron microscopy (TEM) images of a field of nanodiamonds. TEM images (*A*, *B*) and selected-area electron diffraction (*C*) pattern of n-diamonds from Murray Springs (YDB: 426 ppb at 46.5 cm below surface), tilted through 45° (+30° [*A*] through −15° [*B*]). Comparison of various selected objects, such as 1–4, demonstrates that these particles are three-dimensional, rounded to subrounded crystals. A color version of this figure is available online.

tal (2.9 μm long) from the YDB at Arlington Canyon (fig. 15*A*). This is the same lonsdaleite-like grain shown in Kennett et al. (2009*b*) as figures 2*A*–2*C* and S2*B*, referred to above. Figure 15*B* is a TEM image of the same crystal as in panel *A*. Figure 15*C* is an EDS elemental map of the same crystal and shows the composition to be carbon (lighter contrast), with no other elements present.

Figure 16*A* is an HRTEM image showing the same crystal. The double lines define three sets of lattice planes consistent with {10$\bar{1}$0}-type planes of lonsdaleite (prism planes) with a d-spacing of 2.18 Å, as viewed along the [0001] zone axis. Figure 16*B* presents an FFT of an HRTEM image of the same crystal, displaying a spot pattern consistent with the d-spacings for lonsdaleite shown in table D1. The spot pattern matches crystallographic simulations performed for lonsdaleite. Multiple measurements with a calibrated beam (diamond standard) attained an accuracy of approximately ±1%, producing a range of ≈2.16–2.20 Å for the 2.18-Å d-spacing. We also measured d-spacings for commercial graphene and were able to easily distinguish between the d-spacings of 2.18 Å for the lonsdaleite-like crystal and 2.13 Å for graphene, eliminating both graphene or graphane as candidates. Although the lonsdaleite-like crystals may be some other unknown carbon-based mineral,

there is no current evidence that excludes the possibility that it is lonsdaleite.

Rounded Lonsdaleite-Like Crystals. The YDB layer at several sites also contains rounded lonsdaleite-like crystals. Figure 17*A* is a STEM image from the Greenland Ice Sheet near Kangerlussuaq, exhibiting rounded lonsdaleite-like crystals (arrows) mixed with n-diamonds and i-carbon, all ranging from ≈4 to 200 nm in diameter. Figure 17*B* is an HRTEM image of a rounded 10-nm lonsdaleite-like crystal. The EDS results were presented in Kurbatov et al. (2010), confirming that the crystal is carbon, and an EELS spectrum indicated high sp³ bonding, eliminating the possibility that it is graphite, graphene, or graphane. Figure 17*C* is an FFT of an HRTEM image of the same lonsdaleite-like crystal, showing lattice spacings consistent with lonsdaleite.

We also extracted lonsdaleite-like crystals from the YDB layer in several caves. Figure 18*A*, 18*B* shows a 200-nm-long lonsdaleite-like crystal from Sheriden Cave in Ohio. We tilted the TEM stage to confirm that the crystal is three-dimensional and rounded. Figure 18*C* is a STEM image showing a 53-nm-wide object from Daisy Cave on San Miguel Island, one of the Channel Islands located off Santa Barbara, California. Using variable focusing and tilting of the electron beam, we determined that
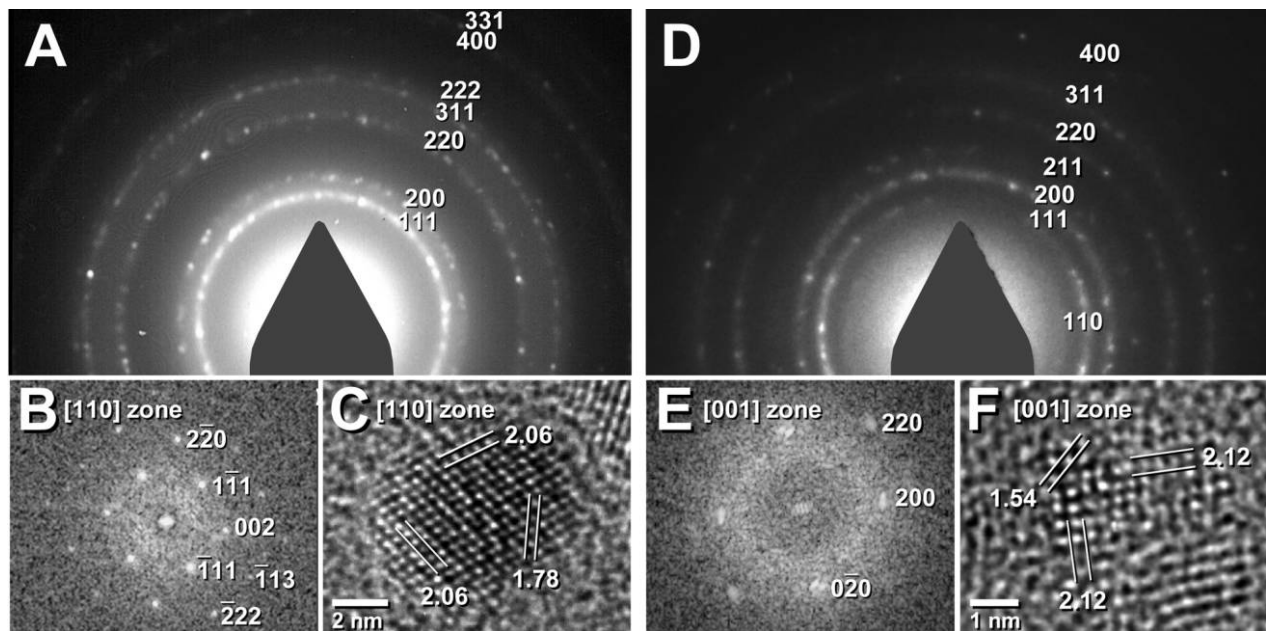
Figure 11. Selected-area electron diffraction (SAD), fast Fourier transform (FFT), and high-resolution transmission electron microscopy (HRTEM) images. *A–C*, SAD pattern (*A*) and FFT (*B*) of the HRTEM image (*C*) of an n-diamond from Murray Springs (Younger Dryas Boundary [YDB]: 426 ppb at 46.5 cm below surface [cmbs]). *D–F*, SAD pattern (*D*) and FFT (*E*) of the HRTEM image (*F*) of i-carbon from Lake Cuitzeo (YDB: 493 ppb at 280 cmbs). Images *B* and *C* are from Israde-Alcántara et al. (2012*b*) and are used with permission. A color version of this figure is available online.

the object is a three-dimensional ball. The EDS analysis indicates that the ball is composed almost solely of carbon, while HRTEM confirms that the matrix is amorphous and studded with a mix of NDs, including one n-diamond star-twin (2.06 Å) and one lonsdaleite-like crystal (2.18- and 1.93-Å d-spacings). We compared that 2.18-Å spacing to the similar 2.13-Å d-spacing for graphene and found that we were able to distinguish them, making it highly unlikely that any of these lonsdaleite-like crystals are graphene. Other than lonsdaleite, no other known carbon allotrope matches all the evidence for these crystals.

Origin of YDB NDs

Multiple explanations have been proposed for the origin of YDB NDs, as follows.

Potential Origin by Cosmic Flux. Cubic NDs are present in meteorites and cosmic dust (Hanneman et al. 1967; Grady et al. 1995; Huss and Lewis 1995), and lonsdaleite is present in some meteorites (Daulton et al. 1996). These observations led Pinter et al. (2011) and others to speculate that YDB microspherules and NDs arrived as components of the gradual, noncatastrophic rain of cosmic debris; if that speculation were correct, those NDs should

display cosmic chemical signatures. Instead, analyses indicate that the isotopic compositions of carbon and nitrogen (δ^{13}C, δ^{15}N, and C/N) in YDB NDs are consistent with a terrestrial origin (Tian et al. 2011; Israde-Alcántara et al. 2012*b*). Those results are supported by Gilmour et al. (1992), who found that δ^{13}C and δ^{15}N values for K-Pg NDs are consistent with formation from terrestrial carbon during the impact itself (Belcher et al. 2005).

Potential Origin from Volcanism or in the Mantle. Cubic diamonds occur in terrestrial deposits, such as kimberlite pipes, which originated from the mantle. Boslough et al. (2012) pointed out that YDB lonsdaleite may originate with terrestrial cubic diamonds because it has been found in a cubic diamond deposit in North Kazakhstan, in Ukrainian titanium placer deposits, in Yakutian diamond placers, and in metamorphosed basaltic rocks on the Kola Peninsula and in the Urals. However, it is unclear whether all of those lonsdaleite examples are terrestrial in origin. For example, Shelkov et al. (1998) presented evidence that lonsdaleite in the Yakutian placers eroded from an impact crater.

Daulton (2012) also suggested that YDB NDs may be derived from mantle material, but isotopic analyses (Tian et al. 2011) are inconsistent with a mantle origin. If such distribution occurred, the
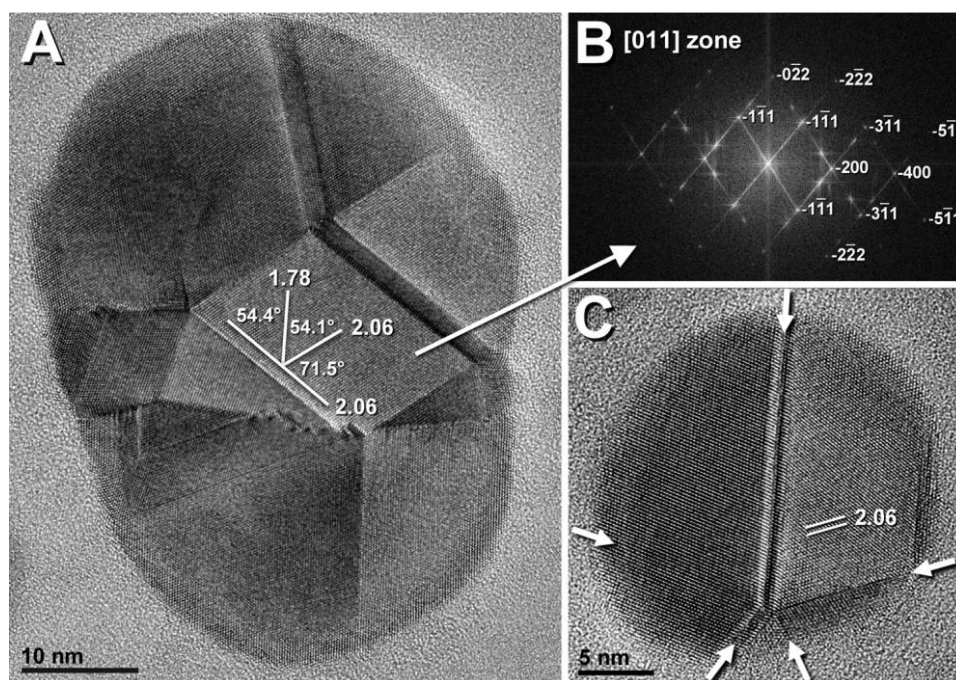
Figure 12. High-resolution transmission electron microscopy (HRTEM) and fast Fourier transform (FFT) images of nanodiamonds (NDs) from Kangerlussuaq, Greenland (Younger Dryas Boundary: 174 ppb at 548 cm below surface). *A*, HRTEM image of an unusually large, multiply twinned n-diamond or flawed cubic ND (53 nm × 39 nm) with 20 conjoined crystals. Center diagram shows typical d-spacings (in Å) and corresponding angles. *B*, FFT of HRTEM image of the central crystal in *A* shows eight d-spacings that are consistent with n-diamond and cubic NDs, when viewed along the [011] zone axis. *C*, HRTEM image of 24-nm-wide n-diamond "star-twin." Arrows are at plane boundaries. Parallel lines indicate d-spacing of 2.06 Å. A color version of this figure is available online.

geochemical signature of the mantle host material should have been detected in more than 700 geochemical analyses conducted on YDB materials (Wittke et al. 2013), and instead, no such signature is apparent. Mantle-derived NDs have never been found in any known geological column associated with coeval peaks in impact markers, arguing against this hypothesis. In any event, terrestrial lonsdaleite has never been observed in any deposits of any age in Europe or North America, where YDB lonsdaleite-like crystals are currently found.

We also considered whether NDs might be produced from volcanic eruptions. To test this, we applied our protocol (see "Material and Methods") to tephra from the Laacher See eruption that occurred near the time of the YDB event. We observed no NDs and no magnetic spherules, eliminating the possibility that this eruption deposited those proxies in the YDB layer.

Potential Origin in Wildfires. Rösler et al. (2005, 2006) and Yang et al. (2008) reported ND-enriched carbon spherules of unknown origin at 70 sites across western Europe, including Germany, Austria, and Belgium. The ND-enriched carbon spher-

ules were found in upper soils, but recently, N. Schryvers (2014, personal communication) was more specific, indicating that their samples were collected from between 10 and 20 cm deep, after removal of topsoil. They wrote that the soils were "modern" but reported no dates. Yang et al. (2008, p. 941) stated that some ND-rich carbon spherules in Germany were found associated with "small-scale crater-like structures," estimated to be ≥1000 yr old, but no craters were associated with the ND-rich carbon spherules in other countries. They added that their origin is unclear but that "an impact related origin ... cannot be ruled out" (p. 941), If so, the age is currently unknown, because near-surface sediments can range in age from modern to millions of years old. As an example, ND-enriched carbon spherules from Gainey (14 cm deep) and Chobot (33 cm deep) were intermixed with Clovis-age tools dating from 13,250–12,800 cal BP (Waters and Stafford 2007). Thus, it is conceivable that some or all of the European near-surface, ND-rich carbon spherules date to the YD onset. Determining the age of the surficial sediments at these sites is necessary to answer these questions.
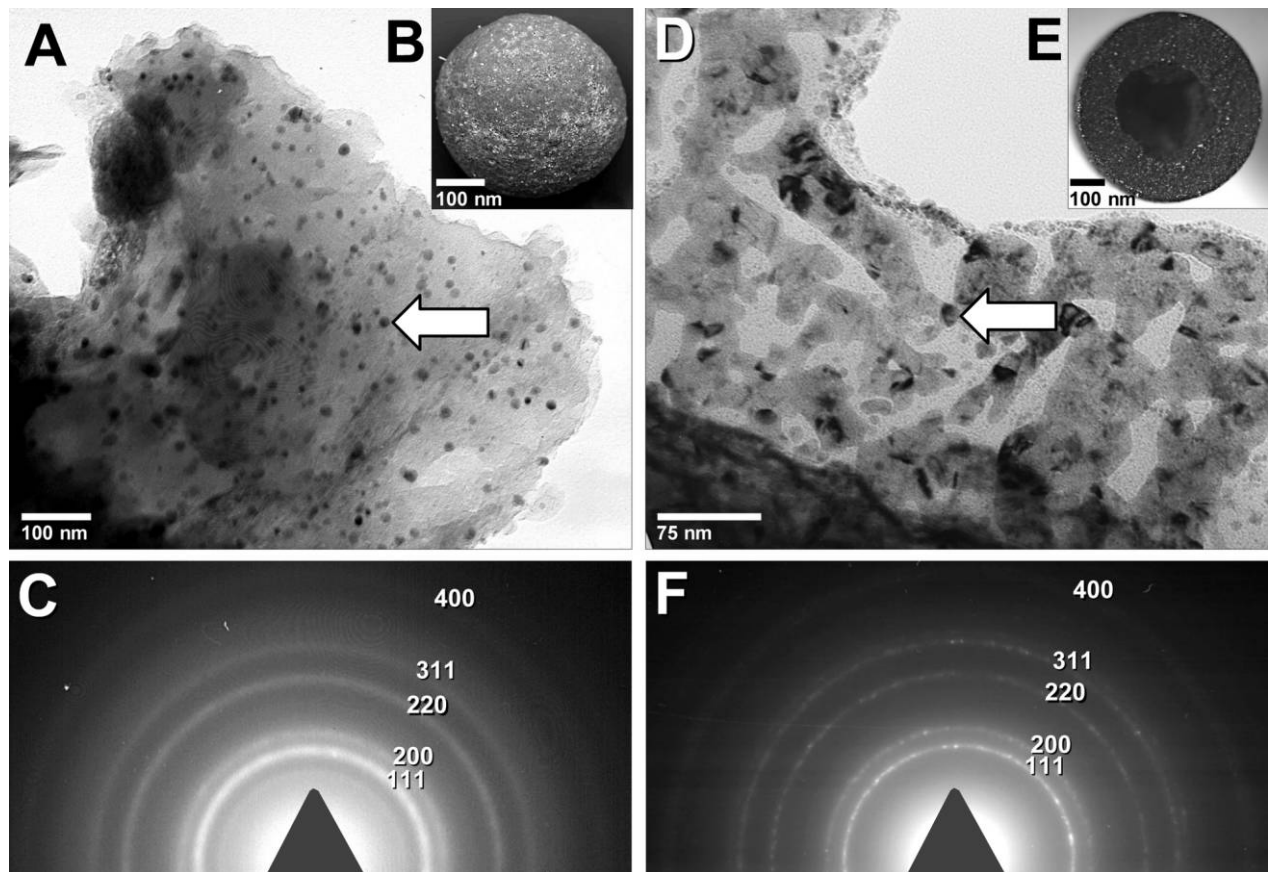
Figure 13. Transmission electron microscopy images (*A*, *B*, *D*, *E*) and selected-area electron diffraction patterns (*C*, *F*) of carbon spherules from Gainey, Michigan (Younger Dryas Boundary [YDB]: 3933 ppb at 30 cm below surface [cmbs]; *A–C*), and Chobot, Alberta, Canada (YDB: 10 ppb at 13.5 cmbs; *D–F*). A color version of this figure is available online.

Van Hoesel et al. (2012, 2014) speculated about a possible wildfire origin for the ND-rich European carbon spherules, on the basis of a recent discovery by Su et al. (2011) that NDs form in candle flames. The NDs are produced at high temperatures (1100°–1300°C) at the anoxic center of the flames, but because NDs combust at ≈400°–600°C in oxygen-rich atmospheres (Hough et al. 1999), they are rapidly destroyed as they approach the flame's oxidation boundary. To protect the NDs from destruction, Su et al. (2011) developed an elaborate procedure using porous aluminum foils to capture and extract the NDs before they could combust. While innovative, this elaborate process does not exist in nature. The particles were identified as "face-centered cubic" NDs, more commonly known as n-diamonds, and there was no evidence of typical, body-centered cubic NDs, as found in the YDB layer.

It is well established that carbon spherules can be produced in intense wildfires involving conifers (Firestone et al. 2007; Israde-Alcántara et al. 2012*b*).

However, no natural wildfires are known to produce NDs inside carbon spherules or other particles. Similarly, no laboratory experiments have been able to produce NDs under conditions that normally appear at Earth's surface. If NDs could be produced in natural fires, which typically recur every 100–1000 yr in any given area, they should be common and ubiquitous in sediments of all ages. Instead, NDs in contiguous stratigraphic horizons are nonexistent to rare (Tian et al. 2011; Bement et al. 2014) and do not correlate with sedimentary layers with high charcoal abundance (Bement et al. 2014). These observations are confirmed by our own work at 22 YDB sites. Similarly, NDs have not been found above or below the K-Pg impact layer (Carlisle and Braman 1991; Gilmour et al. 1992; Bunch et al. 2008), even though biomass burning is accepted as having been broadly pervasive over the K-Pg boundary interval (Wolbach 1990).

In summary, there is no evidence for and no known process for production of NDs in natural
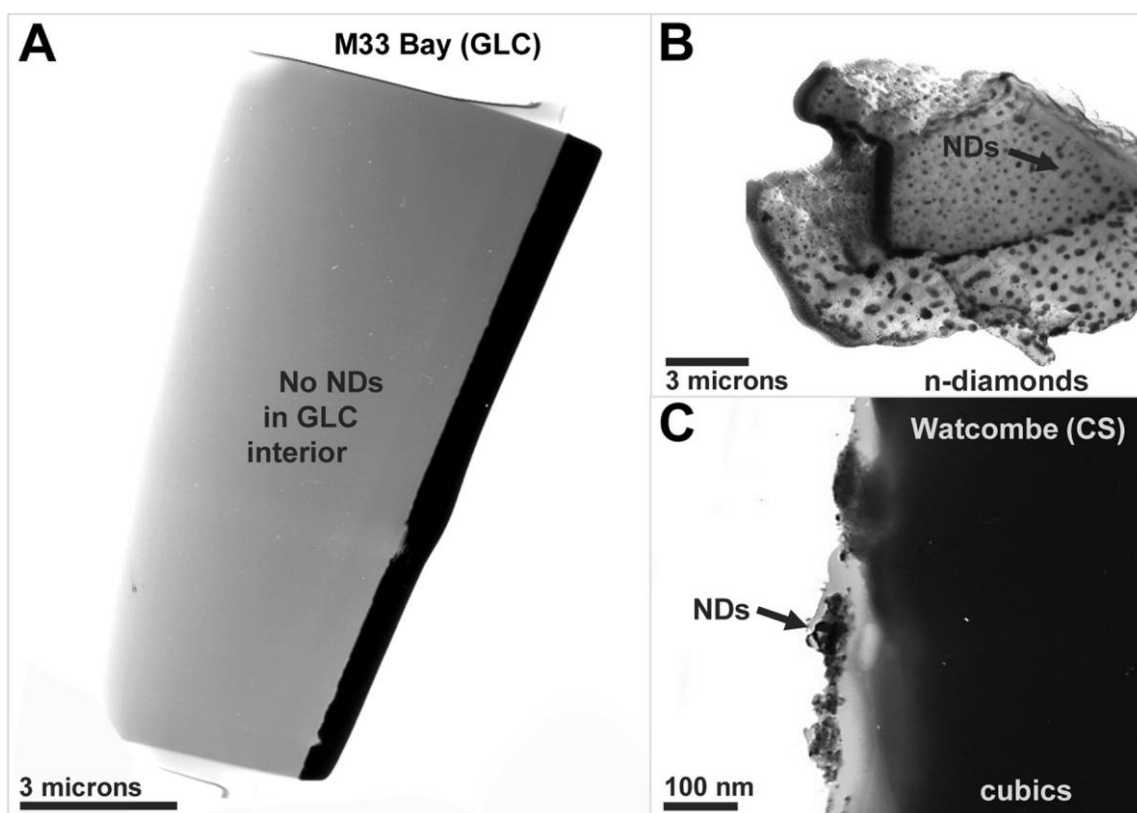
Figure 14. Transmission electron microscopy (TEM) images of nanodiamonds (NDs) in glass-like carbon (GLC) and carbon spherules (CS). *A*, TEM image from M33 Bay, Myrtle Beach, South Carolina (40 cm below surface [cmbs]); the sectioned GLC displays only amorphous carbon and no NDs (the dark crust is mounting material). *B*, TEM image of a flake from the surface of the GLC in *A*; selected-area electron diffraction patterns reveal a high abundance of n-diamonds. *C*, TEM image from Watcombe Bottom, United Kingdom (Younger Dryas Boundary: 130 ppb at 65 cmbs) shows a thin zone of cubic NDs along one edge of a fragment of a carbon spherule. A color version of this figure is available online.

wildfires. This argues against biomass burning as the source of the assemblage of NDs in the YDB or other sedimentary sequences.

Potential Origin within Sclerotia. Scott et al. (2010) and Hardiman et al. (2012) stated that all carbon spherules from Arlington Canyon and other sites are simply either charred fecal pellets or fungal sclerotia. To be viable, the sclerotial hypothesis must account for the presence of millions of NDs entrained within each carbon spherule (Kennett et al. 2009*a*). There is no credible mechanism by which fungi can create NDs in sclerotia, but we considered whether NDs might have adhered to preexisting sclerotia while colocated in YDB sediment. For comparison, the average sedimentary abundance of NDs is ≈200 ppb, whereas the ND concentrations in carbon spherules is >35% at three sites, a difference of more than one million times. There is no plausible process by which sclerotia could extract NDs from surrounding sediment,

concentrate them a million times, and do so only at one time during the past 13,000 yr. Thus, the best explanation is that ND-rich carbon spherules derive from conifers that were incinerated by the impact event (Israde-Alcántara et al. 2012*b*).

Potential Origin from Lightning. We considered whether diamonds might form during high-temperature lightning strikes. To evaluate this, we applied the protocol to extract potential NDs from a collection of fulgurites but observed not even one ND. Furthermore, Wittke et al. (2013) studied remanent magnetism in YDB impact spherules that are closely associated with NDs. They found no evidence for lightning strikes in YDB sediment, thus arguing against this hypothesis.

Potential Origin as Anthropogenic NDs. Rösler et al. (2006) and Bement et al. (2014) discovered NDs in deposits near the ground surface. We investigated the possibility that modern anthropogenic ac-
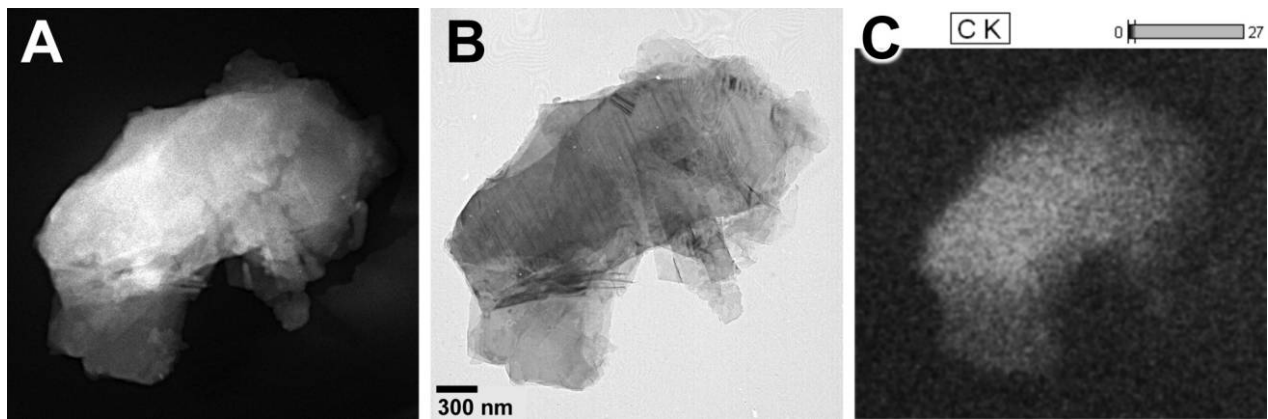
Figure 15. Younger Dryas Boundary lonsdaleite-like crystal. *A*, Scanning transmission electron microscopy image from Arlington Canyon, California (1760 ppb at 462 cm below surface). *B*, Transmission electron microscopy images of same crystal. *C*, Corresponding energy dispersive X-ray spectrometry elemental carbon map of the crystal; no other elements were detected. Images from Kennett et al. (2009*b*); used with permission. A color version of this figure is available online.

tivities might produce synthetic NDs that migrated downward to the YDB. We examined fly ash residue from a modern New Jersey power plant that incinerates coal at high temperatures under anoxic conditions, similar to some laboratory conditions that produce NDs. We found abundant graphene but no NDs and no melt-glass containing high-temperature, melted quartz. Furthermore, some YDB NDs are found up to ≈5 m below surface but not in intervening layers, making it unlikely that they migrated downward from the surface. In addition, we found no detectable NDs in surficial sediments investigated at eight sites (fig. 2; table D4). All these findings argue against the hypothesis that NDs are produced through anthropogenic activities and are common in surface and other sediments.

Potential Origin by Cosmic Impact. Cubic NDs have been reported at the K-Pg boundary (Gilmour et al. 1992; Hough et al. 1997), and Israde-Alcántara et al. (2012*b*) reported that YDB NDs are morphologically and compositionally similar to those in
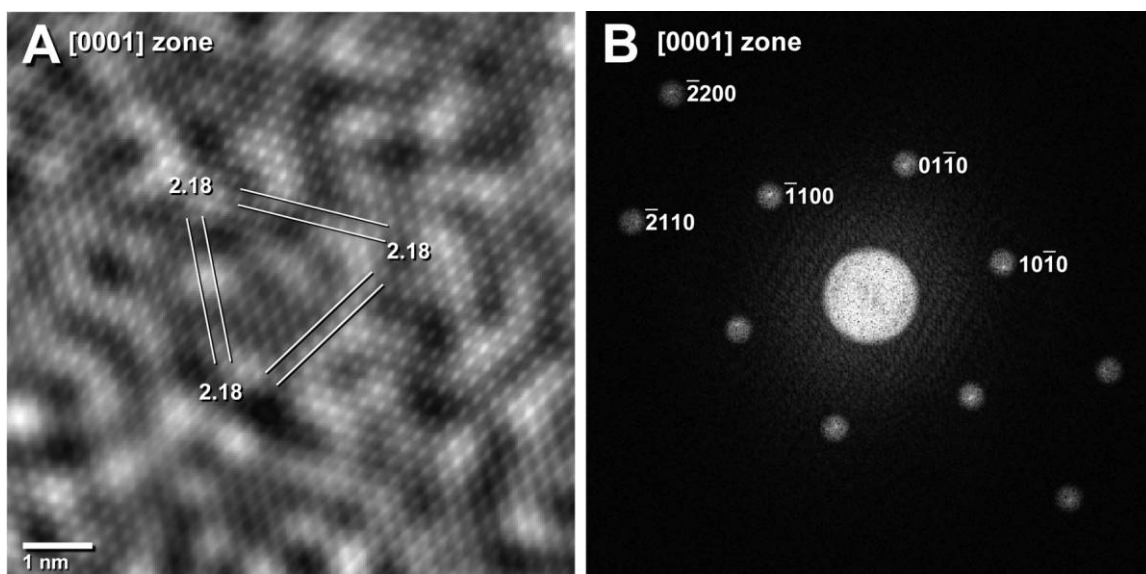

Figure 16. Younger Dryas Boundary (YDB) lonsdaleite-like crystal from Arlington Canyon (1760 ppb at 462 cm below surface). *A*, High-resolution transmission electron microscopy of the crystal; *B*, corresponding fast Fourier transform. A color version of this figure is available online.
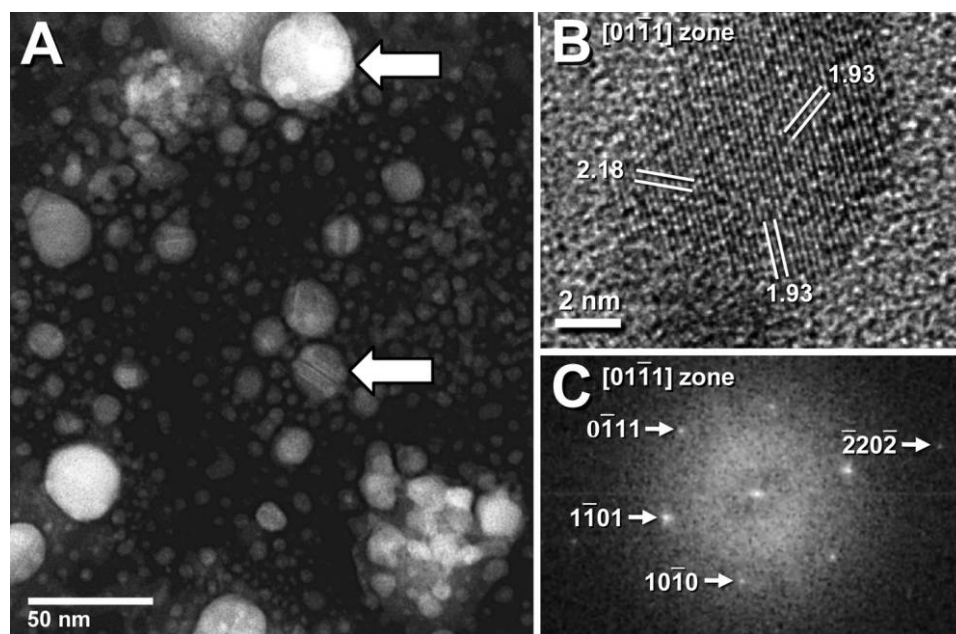
Figure 17. Scanning transmission electron microscopy (STEM) and high-resolution transmission electron microscopy (HRTEM) images of lonsdaleite-like crystals. *A*, STEM image of group of lonsdaleite-like crystals (arrows) mixed with other NDs, from Kangerlussuaq (Younger Dryas Boundary [YDB]: 174 ppb at 548 cm below surface [cmbs]). *B*, HRTEM image of a 10-nm lonsdaleite-like monocrystal from Lake Cuitzeo (YDB: 493 ppb at 280 cmbs); one (10$\bar{1}$1) plane with a spacing of 1.93 Å is visible, along with the (10$\bar{1}$0) plane at 2.18 Å, consistent with lonsdaleite. *C*, Fast Fourier transform of an HRTEM image of the same crystal as in *B*, with d-spacings along the [01$\bar{1}$1] zone axis, revealing one (10$\bar{1}$0) plane with a lattice spacing of 2.18 Å and two (10$\bar{1}$1) planes with lattice spacings of 1.93 Å. A color version of this figure is available online.

the K-Pg (Kennett et al. 2009*a*, 2009*b*; Kurbatov et al. 2010). Angular lonsdaleite crystals also formed in some impact events via shock metamorphism of graphite in the target rocks (Hough et al. 1997; Koeberl et al. 1997; Langenhorst et al. 1998; DeCarli et al. 2002; Oleinik et al. 2003). Lonsdaleite grains have been reported in impact events, e.g., Ries Crater, the K-Pg event (Bunch et al. 2008), and the 1908 Tunguska airburst in Siberia (Bunch et al. 2008; Kvasnytsya et al. 2013). Although lonsdaleite is known to be formed through shock metamorphism during surface impacts, its presence at the site of the Tunguska airburst indicates that it also can form during cosmic airbursts. This is demonstrated in laboratory experiments (Miura and Okamoto 1997), in which a high-velocity impact into a limestone target produced carbon vapor that condensed into graphite inside a high-temperature, reducing vapor plume. Subsequently, lonsdaleite and cubic NDs formed when the carbon plume reacted with water ice, creating oxidizing conditions. This demonstrates that lonsdaleite can form through a process similar to carbon vapor deposition (CVD), es-

pecially if the YDB impactor struck the ice sheet or oceans, as proposed by Firestone et al. (2007).

Criticism of an impact origin for the YDB has included an apparent absence of an impact crater (Boslough et al. 2012). However, this position contradicts a broad consensus among impact researchers, including some of those coauthors, that some impact events lack known craters or that the craters remain undiscovered (Boslough and Crawford 2008). Some examples are the Tunguska airburst debris field ($\approx$2 $\times$ 10^3 km^2), the Libyan glass field ($\approx$2 $\times$ 10^3 km^2), the Dakhleh glass field ($\approx$1 $\times$ 10^3 km^2), and the Australasian tektite field ($\approx$5 $\times$ 10^7 km^2, or 10% of the planet). This apparent lack of cratering has been variously explained. Some impacts were hypothesized to have been airbursts, or alternately, some events formed craters that have yet to be found (Boslough and Crawford 2008), as may be the case with the YDB impact. Regardless, these widely accepted, craterless impact events deposited up to millions of tons of spherules, meltglass, and NDs across up to $\approx$10% of Earth.
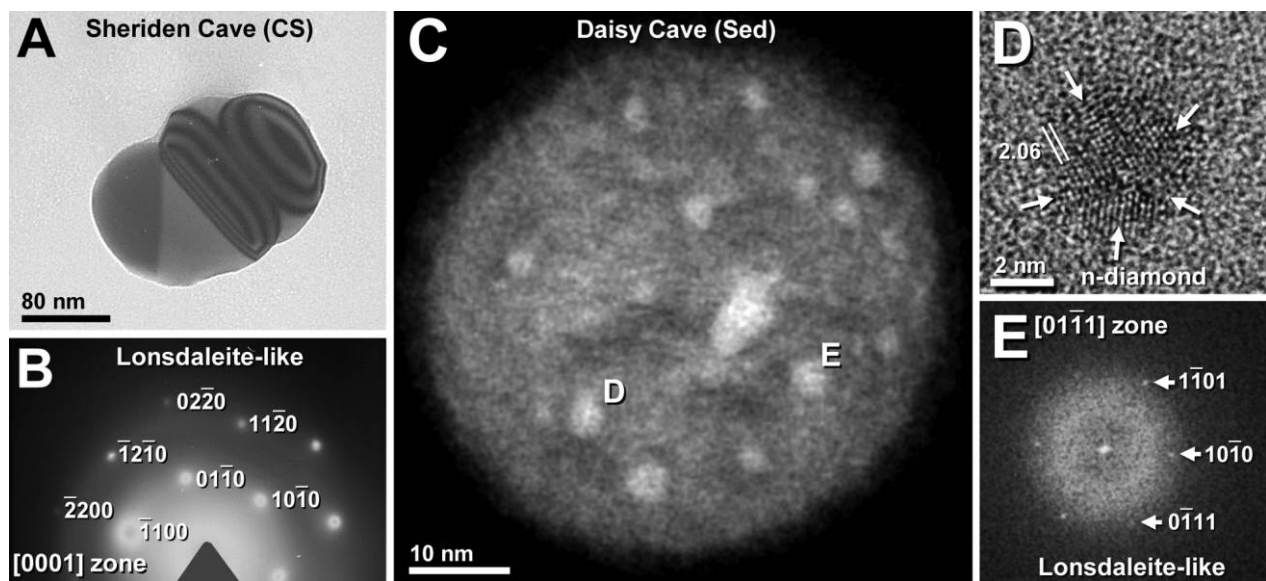
There are only two known layers, broadly dis-

Figure 18. Younger Dryas Boundary lonsdaleite-like crystals from two caves. *A*, *B*, Transmission electron microscopy (*A*) and selected-area electron diffraction (*B*) images of 200-nm-long, three-dimensional, lonsdaleite-like crystal from Sheriden Cave, Ohio (108 ppb at 45.3 cm below surface [cmbs]), as viewed along the [0001] zone axis. *C*, Scanning transmission electron microscopy image of 53-nm, three-dimensional carbon spherule containing n-diamonds and lonsdaleite-like crystals, from Daisy Cave, California (100 ppb at 80 cmbs). *D*, High-resolution transmission electron microscopy (HRTEM) image of the nanodiamond marked "D" in *C*; arrows define common lattice planes. *E*, Fast Fourier transform of an HRTEM image of another nanocrystal, marked "E" in *C*, showing d-spacings consistent with lonsdaleite when viewed along the [01$\bar{1}$1] zone axis, revealing one (10$\bar{1}$0) plane with a lattice spacing of 2.18 Å and two (10$\bar{1}$1) planes with lattice spacings of 1.93 Å. CS = carbon spherule; Sed = sediment. A color version of this figure is available online.

tributed across several continents, that exhibit co-eval abundance peaks in a comprehensive assemblage of cosmic-impact markers, including NDs, high-temperature quenched spherules, high-temperature melt-glass (1730° to >2200°C), carbon spherules, iridium, and aciniform carbon. One of those layers is at the K-Pg impact boundary, and the other is at the YDB. Other events, such as the Chesapeake Bay and Popigai craters, include a nearly complete assemblage, but some markers are missing, possibly because no one has searched for them. This unique assemblage of proxies has never been reported to result from meteoritic flux, wildfires, volcanism, or any other nonimpact process. At present, a cosmic-impact event is the only known mechanism capable of distributing NDs and the complete assemblage of YDB proxies across multiple continents.

How NDs Might Form in a Cosmic Impact. Hough et al. (1997) suggested that the K-Pg NDs formed by the CVD process, which requires a source of carbon vapor and the reducing atmosphere of the fireball (Wen et al. 2007). For the K-Pg, it is proposed that the NDs formed when the impactor collided with carbon-rich Yucatan bedrock, e.g., limestones and dolostones containing hydrocarbons (Belcher et al. 2005). In a related discovery, hydrocarbons in some oil fields adjacent to the crater in Yucatan contain n-diamonds and are proposed to have formed during the K-Pg impact event (Santiago et al. 2004).

Synthetic cubic NDs, n-diamonds, and i-carbon are produced by many industrial or laboratory processes, 14 of which are listed in table D5 (Wen et al. 2007). In addition to a source of carbon, the production of these NDs requires the presence of at least two of the following conditions: high temperatures, high pressures, and low- to zero-oxygen (anoxic) atmospheres. Regarding temperature, 11 of the 14 processes require high temperatures of up to 3400°C, beyond the normal range observed in nature. Four of the processes require high pressures of ≈14–70 GPa that are well beyond typical natural processes. Four involve near-vacuum conditions unknown at Earth's surface, and nine require oxygen-free, reducing atmospheres (e.g., argon, hydrogen) that do not support combustion, as required for wildfires. Ten call for exotic processes, such as plasma jets, lasers, microwave beams, catalysts, and/or strong magnetic

fields, that do not exist in nature. Furthermore, nine of these processes yield only n-diamonds and i-carbon and not cubic NDs or lonsdaleite. Thus, in every known case of industrial production, the requisite conditions do not occur in nature but do occur during a cosmic-impact event.

During our experiments investigating formation mechanisms, we discovered that NDs are commonly present in commercially produced activated carbon from both Norit and Calgon Carbon. Produced at ≈1000°C in a low-oxygen steam atmosphere, the activated carbon contains n-diamonds and i-carbon but no cubics or lonsdaleite. The feedstock used for production of NDs is charcoal that is usually charred from wood at ≈500°C, and our analyses indicate that the charcoal does not contain any NDs before or after charring. Later, during an activation process that uses superheated steam (≈1000°C), the NDs grow within the activated carbon at abundances similar to those found in YDB carbon spherules (fig. C7). In multiple experiments duplicating the commercial process, we demonstrated that formation of these NDs requires exotic atmospheres (steam, argon, or CO_2) combined with temperatures of 1000°–1200°C, similar to other industrial processes that yield NDs (table D5). The conditions required to produce NDs in activated carbon mimic those in a cosmic impact, e.g., anoxia and high temperatures.

Regarding the formation of lonsdaleite, industrial diamond research has been underway for nearly 50 yr, since lonsdaleite was first synthesized with explosives in 1966 by one of us (DeCarli 1966). The process is similar to shock-formation conditions in a cosmic-impact event, during which lonsdaleite typically forms from the high-pressure transformation of graphite. However, synthetic lonsdaleite can also be produced under nonshock conditions, e.g., by growth in a hydrogen plasma jet in a CVD-like process (Maruyama et al. 1992) and by enhancement of carbon in silicon carbide wafers (Gogotsi et al. 2001; Welz et al. 2006; table D5). These other processes suggest that lonsdaleite could form without physical shock at high temperatures in the fireball of a cosmic-impact event. If so, the lonsdaleite-like crystals that we have observed may have formed that way.

The CVD-like production of NDs is proposed to occur in extrasolar material (Daulton et al. 1996), most likely during the explosion of a carbon-rich star. Several studies have speculated that YDB NDs may have formed through CVD (Tian et al. 2011; van Hoesel et al. 2012, 2014), although they offered no evidence as to whether such a process could occur independently of an impact. The plausibility of an impact-related source for the YDB NDs is supported by the fact that requisite conditions for ND formation by CVD in the laboratory and space (a carbon source and anoxia) also occur in an impact fireball.

In a related discovery in the YDB layer in Belgium, Tian et al. (2011) found "carbon onions," which are nanosized objects formed from concentric shells of carbon. They noted that NDs can form within carbon onions under anoxic conditions in the laboratory and speculated that the carbon onions might serve as nanometer-sized pressure cells for YDB ND formation. Later, van Hoesel et al. (2012) remarked that cubic diamonds form alongside carbon onions in wood experimentally charred at 700°C and cooled in an anoxic (nitrogen) atmosphere. However, those conditions are unlike those in wildfires or other terrestrial processes but are similar to the ones in an impact/airburst. Israde-Alcántara et al. (2012b) also reported carbon onions, some apparently containing nanocrystals, and proposed that the requisite conditions could occur during an impact. One possible mechanism is that the thermal radiation from the air shock at ≈20,000°C could flash-pyrolyse vegetation to provide available elemental carbon, after which reactions with the atmosphere would locally deplete the oxygen, permitting formation of NDs from carbon vapor.

Future Work. It is important to continue investigating the origin of YDB NDs, especially of lonsdaleite-like crystals, because lonsdaleite has been considered an important proxy for cosmic impact. It would also be useful to use Raman spectroscopy for more thorough characterization of YDB NDs, although this would require the extraction of a far larger quantity of NDs (approx. >10 mg of each sample). Adequate quantities are more readily available from the margin of the Greenland Ice Sheet, where large amounts of ice can be extracted from the exposed YDB layer (Kurbatov et al. 2010).

Conclusions

We have presented a detailed protocol for isolating YDB NDs, requiring the use of numerous reagents. The identification of the isolated NDs involves two main methods, electron microscopy imaging and electron spectroscopy, using up to nine imaging, analytical, or quantification procedures: scanning electron microscopy, STEM, TEM, HRTEM, EDS, SAD, FFT, EELS, and EFTEM. The entire procedure is labor-intensive and technically demanding. Even so, it has proven to be effective and replicable by skilled independent groups, based on the processing of more than 100 samples. The presence of NDs at 24 sites in 10 countries on three continents, in-

cluding results from six independent groups, is strong evidence for the existence of YDB abundance peaks in NDs.

Analysis of YDB dates indicates that 18 of 24 sites, including the Aalsterhut and Arlington Canyon sites, are statistically part of the same population, with ages falling within the proposed YDB age range of 12,800 ± 150 (12,950–12,650) cal BP. These ages also correspond to the onset of YD climate change in the GISP2 ice core within an age range of 12,892 ± 260 (13,152–12,632) b2k, consistent with the hypothesis that the cosmic impact triggered that cooling event. The YDB layer has been found on each of the four continents currently investigated.

Some researchers have proposed that YDB NDs originated from wildfires, volcanism, the mantle, and/or by unknown processes that are coincidentally coeval, but those hypotheses can be rejected because each fails to account for the entire assemblage of proxies. Numerous accepted impact events display the same evidence as found at the YDB, and the YDB and the K-Pg impact layers contain the only known multicontinental, coeval abundance peaks in the entire assemblage of proxies within the past 65 m.yr. Of all the proposed hypotheses, a cosmic-impact event at the onset of the YD cooling episode is the only hypothesis capable of explaining the simultaneous deposition of peak abundances in NDs, magnetic and glassy spherules, melt-glass, platinum, and/or other proxies across at least four continents ($\approx$50 million km^2). The evidence strongly supports a major cosmic-impact event at 12,800 ± 150 cal BP.

Author Affiliations

1. Department of Chemistry, DePaul University, Chicago, Illinois 60614, USA; 2. Department of Environmental Health Sciences/UCLA Center for Occupational and Environmental Health, University of California, Los Angeles, California 90095, USA; 3. National Institute for Materials Science, Tsukuba 305-0047, Japan; 4. Center for Advanced Materials Characterization at Oregon, University of Oregon, Eugene, Oregon 97403, USA; 5. Department of Anthropology, Pennsylvania State University, University Park, Pennsylvania 16802, USA; 6. SRI International, Menlo Park, California 94025, USA; 7. Geology Program, School of Earth Science and Environmental Sustainability, Northern Arizona University, Flagstaff, Arizona 86011, USA; 8. Departamento de Geología y Mineralogía, Edificio U-4, Instituto de Ciencias de la Tierra, Universidad Michoacana de San Nicolás de Hidalgo, C.P. 58060, Morelia, Michoacán, Mexico; 9. US Geological Survey, Menlo Park, California 94025, USA; 10. South Carolina Institute of Archaeology and Anthropology, University of South Carolina, Columbia, South Carolina 29208, USA; 11. Departments of Anthropology and Geology, University of Cincinnati, Cincinnati, Ohio 45221, USA; 12. Kimstar Research, Fayetteville, North Carolina 28312, USA; 13. Museum of Natural and Cultural History, University of Oregon, Eugene, Oregon 97403, USA; 14. AMS [14]C Dating Centre, Department of Physics and Astronomy, University of Aarhus, Ny Munkegade 120, Aarhus, Denmark; and Centre for GeoGenetics, Natural History Museum of Denmark, Geological Museum, Oester Voldgade 5-7, DK-1350 Copenhagen, Denmark; 15. Exploration Geologist, 1016 NN, Amsterdam, The Netherlands; 16. College of Liberal Arts, Rochester Institute of Technology, Rochester, New York 14623, USA; 17. Lawrence Berkeley National Laboratory, Berkeley, California 94720, USA; 18. Departament de Prehistòria i Arqueologia, Universitat de València, Avenida Blasco Ibáñez 28, E-46010 Valencia, Spain; 19. Departamento de Prehistoria y Arqueología, Facultad de Geografía e Historia, Universidad Nacional de Educación a Distancia, Paseo Senda del Rey 7, E-28040 Madrid, Spain; 20. GeoScience Consulting, Dewey, Arizona 86327, USA; 21. Department of Earth Science and Marine Science Institute, University of California, Santa Barbara, California 93106, USA.

REFERENCES CITED

Baker, D. W.; Miranda, P. J.; and Gibbs, K. E. 2008. Montana evidence for extra-terrestrial impact event that caused ice-age mammal die-off. Eos Trans. Am. Geophys. Union 89(23), Jt. Assem. Suppl., Abstract P41A-05.

Belcher, C. M.; Collinson, M. E.; and Scott, A. C. 2005. Constraints on the thermal energy released from the Chicxulub impactor: new evidence from multi-method charcoal analysis. J. Geol. Soc. Lond. 162:591–602.

Bement, L. C.; Madden, A. S.; Carter, B. J.; Simms, A. R.; Swindle, A. L.; Alexander, H. M.; Fine, S.; and Benemara, M. 2014. Quantifying the distribution of nanodiamonds in pre-Younger Dryas to recent age deposits along Bull Creek, Oklahoma Panhandle, USA. Proc. Natl. Acad. Sci. USA. 111:1726–1731. doi:10.1073/pnas.1309734111.

Berger, S. D.; McKenzie, D. R.; and Martin, P. J. 1988. EELS analysis of vacuum arc-deposited diamond-like films. Philos. Mag. Lett. 57:285–290.

Blaauw, M.; Holliday, V. T.; Gill, J. L.; and Nicoll, K. 2012. Age models and the Younger Dryas impact hypothesis. Proc. Natl. Acad. Sci. USA 109:E2240. doi:10.1073/pnas.1206143109.

Boslough, M.; Nicoll, K.; Holliday, V.; Daulton, T. L.; Meltzer, D.; Pinter, N.; Scott, A. C.; et al. 2012. Arguments and evidence against a Younger Dryas impact event. In Giosan, L.; Fuller, D. Q.; Nicoll, K.; Flad, R. K.; and Clift, P. D., eds. Climates, landscapes, and civilizations. Geophys. Monogr. Ser. 198:13–26.

Boslough, M. B. E., and Crawford, D. A. 2008. Low-altitude airbursts and the impact threat. Int J. Impact Eng. 35:1441–1448.

Brauer, A.; Haug, G. H.; Dulski, P.; Sigman, D. M.; and Negendank, J. F. W. 2008. An abrupt wind shift in western Europe at the onset of the Younger Dryas cold period. Nat. Geosci. 1:520–523.

Bronk Ramsey, C. 2009. Bayesian analysis of radiocarbon dates. Radiocarbon 51:337–360.

Bunch, T. E.; Hermes, R. E.; Moore, A. M. T.; Kennett, D. J.; Weaver, J. C.; Wittke, J. H.; DeCarli, P. S.; et al. 2012. Very high-temperature impact melt products as evidence for cosmic airbursts and impacts 12,900 years ago. Proc. Natl. Acad. Sci. USA 109:E1903–E1912.

Bunch, T. E.; Schultz, P. H.; Wittke, J. H.; West, A.; Kennett, J. P.; and Kennett, D. J. 2009. Summary of impact markers and potential impact mechanisms for the YDB impact event at 12.9 ka. Eos Trans. Am. Geophys. Union 90(52), Fall Meet. Suppl., Abstract PP33B-10.

Bunch, T. E.; Wittke, J. H.; West, A.; Kennett, J. P.; Kennett, D. J.; Que Hee, S. S.; Wolbach, W. S.; Stich, A.; Mercer, C.; and Weaver, J. C. 2008. Hexagonal diamonds (lonsdaleite) discovered in the K/T impact layer in Spain and New Zealand. Eos Trans. Am. Geophys. Union 89(53), Fall Meet. Suppl., Abstract PP13C-1476.

Carlisle, D. B., and Braman, D. R. 1991. Nanometre-size diamonds in the Cretaceous/Tertiary boundary clay of Alberta. Nature 352:708–709.

Courty, M.-A.; Crisci, A.; Fedoroff, M.; Grice, K.; Greenwood, P.; Mermoux, M.; Smith, D.; and Thiemens, M. 2008. Regional manifestation of the widespread disruption of soil-landscapes by the 4 kyr BP impact-linked dust event using pedo-sedimentary micro-fabrics. In Kapur, S.; Mermut, A.; and Stoops, G., eds. New trends in soil micromorphology. Berlin, Springer, p. 211–236.

Daulton, T. L. 2012. Suspect cubic diamond "impact" proxy and a suspect lonsdaleite identification. Proc. Natl. Acad. Sci. USA 109:E2242.

Daulton, T. L.; Eisenhour, D. D.; Bernatowicz, T. J.; Lewis, R. S.; and Buseck, P. R. 1996. Genesis of presolar diamonds: comparative high-resolution transmission electron microscopy study of meteoritic and terrestrial nano-diamonds. Geochim. Cosmochim. Acta 60:4853–4872.

Daulton, T. L.; Pinter, N.; and Scott, A. 2010. No evidence of nanodiamonds in Younger-Dryas sediments to support an impact event. Proc. Natl. Acad. Sci. USA 107:16,043–16,047.

de Araujo, P. L. B.; Mansoori, G. A.; and de Araujo, E. S. 2012. Diamondoids: occurrence in fossil fuels, applications in petroleum exploration and fouling in petroleum production. A review paper. Int. J. Oil Gas Coal Technol. 5:316–367.

DeCarli, P. S. 1966. Method of making diamond. U.S. Patent 3,238,019, filed October 1.

DeCarli, P. S.; Bowden, E.; Jones, A. P.; and Price, G. D. 2002. Laboratory impact experiments versus natural impact events. In Koeberl, C., and MacLeod, K., eds. Catastrophic events and mass extinctions: impacts and beyond. Geol. Soc. Am. Spec. Pap. 356:595–605.

Demitroff, M.; LeCompte, M. A.; and Rock, B. N. 2009. Cold climate related structural sinks accommodate unusual soil constituents, Pinelands National Reserve, New Jersey, USA. Eos Trans. Am. Geophys. Union 90(52), Fall Meet. Suppl., Abstract PP31D-1394.

Fawcett, P. J., and Boslough, M. B. E. 2002. Climatic effects of an impact-induced equatorial debris ring. J. Geophys. Res. 107(D15):ACL 2-1–ACL 2-18.

Fayek, M.; Anovitz, L. M.; Allard, L. F.; and Hull S. 2012. Framboidal iron oxide: chondrite-like material from the black mat, Murray Springs, Arizona. Earth Planet. Sci. Lett. 319/320:251–258.

Firestone, R. B. 2009. The case for the Younger Dryas extraterrestrial impact event: mammoth, megafauna, and Clovis extinction, 12,900 years ago. Cosmology 2:256–285.

Firestone, R. B.; West, A.; Kennett, J. P.; Becker, L.; Bunch, T. E.; Revay, Z. S.; Schultz, P. H.; et al. 2007. Evidence for an extraterrestrial impact 12,900 years ago that contributed to the megafaunal extinctions and the

Younger Dryas cooling. Proc. Natl. Acad. Sci. USA 104:16,016–16,021.

Gilmour, I.; Russell, S. S.; Arden, J. W.; Lee, M. R.; Franchi, I. A.; and Pillinger, C. T. 1992. Terrestrial carbon and nitrogen isotopic ratios from Cretaceous-Tertiary boundary nanodiamonds. Science 258:1624–1626.

Gogotsi, Y.; Welz, S.; Ersoy, D. A.; and McNallan, M. J. 2001. Conversion of silicon carbide to crystalline diamond-structured carbon at ambient pressure. Nature 411:283–287.

Grady, M. M.; Lee, M. R.; Arden, J. W.; and Pillinger, C. T. 1995. Multiple diamond components in Acfer 182. Earth Planet. Sci. Lett. 136:677–692.

Hanneman, R. E.; Strong, H. M.; and Bundy, F. P. 1967. Hexagonal diamonds in meteorites: implications. Science 155:995–997.

Hardiman, M.; Scott, A. C.; Collinson, M. E.; and Anderson, R. S. 2012. Inconsistent redefining of the carbon spherule "impact" proxy. Proc. Natl. Acad. Sci. USA 109:E2244. doi:10.1073/pnas.1206108109.

Haynes, C. V., Jr.; Boerner, J.; Domanik, K.; Lauretta, D.; Ballenger, J.; and Goreva, J. 2010. The Murray Springs Clovis site, Pleistocene extinction, and the question of extraterrestrial impact. Proc. Natl. Acad. Sci. USA 107:4010–4015.

Haynes, C. V., Jr., and Huckell, B. B., eds. 2007. Murray Springs: a Clovis site with multiple activity areas in the San Pedro Valley, Arizona. University of Arizona Press, Tucson, 288 p.

Heymann, D.; Cataldo, F.; Pontier-Johnson, M.; and Rietmeijer, F. J. M. 2006. Fullerenes and related structural forms of carbon in chondritic meteorites and the moon. *In* Rietmeijer, F. J. M., ed. Natural fullerenes and related structures of elemental carbon. Springer, Dordrecht, p.145–189.

Hough, R. M.; Gilmour, I.; and Pillinger, C. T. 1999. Carbon isotope study of impact diamonds in Chicxulub ejecta at Cretaceous-Tertiary boundary sites in Mexico and the western interior of the United States. *In* Dressler, B. O., and Sharpton, V. L.; eds., Large meteorite impacts and planetary evolution II. Geol. Soc. Am. Spec. Pap. 339:215–222.

Hough, R. M.; Gilmour, I.; Pillinger, C. T.; Langenhorst, F.; and Montanari, A. 1997. Diamonds from the iridium-rich K-T boundary layer at Arroyo el Mimbral, Tamaulipas, Mexico. Geology 25:1019–1022.

Hu, M.; Tian, F.; Zhao, Z.; Huang, Q.; Xu, B.; Wang, L.-M.; Wang, H.-T.; Tian, Y.; and He, J. 2012. Exotic cubic carbon allotropes. J. Phys. Chem. C 116:24,233–24,238.

Huss, G. R., and Lewis, R. S. 1995. Presolar diamond, SiC, and graphite in primitive chondrites: abundances as a function of meteorite class and petrologic type. Geochim. Cosmochim. Acta 59:115–160.

Israde-Alcántara, I.; Bischoff, J. L.; DeCarli, P. S.; Domínguez-Vázquez, G.; Bunch, T. E.; Firestone, R. B.; Kennett, J. P.; and West, A. 2012*a*. Reply to Blaauw et al., Boslough, Daulton, Gill et al., and Hardiman et al.: Younger Dryas impact proxies in Lake Cuitzeo, Mexico. Proc. Natl. Acad. Sci. USA 109:E2245–E2247.

Israde-Alcántara, I.; Bischoff, J. L.; Domínguez-Vázquez,

G.; Li, H.-C.; DeCarli, P. S.; Bunch, T. E.; Wittke, J. H.; et al. 2012*b*. Evidence from Central Mexico supporting the Younger Dryas extraterrestrial impact hypothesis. Proc. Natl. Acad. Sci. USA 109:E738–E747.

Ives, J. W., and Froese, D. G. 2013. The Chobot site (Alberta, Canada) cannot provide evidence of a cosmic impact 12,800 y ago. Proc Natl. Acad. Sci. USA 110:E3899.

Kennett, D. J.; Kennett, J. P.; West, A.; Mercer, C.; Que Hee, S. S.; Bement, L.; Bunch, T. E.; Sellers, M.; and Wolbach, W. S. 2009*a*. Nanodiamonds in the Younger Dryas boundary sediment layer. Science 323:94.

Kennett, D. J.; Kennett, J. P.; West, A.; West, G. J.; Bunch, T. E.; Culleton, B. J.; Erlandson, J. M.; et al. 2009*b*. Shock-synthesized hexagonal diamonds in Younger Dryas boundary sediments. Proc. Natl. Acad. Sci. USA 106:12,623–12,628.

Koeberl, C.; Masaitis, V. L.; Shafranovsky, G. I.; Gilmour, I.; Langenhorst, F.; and Schrauder, M. 1997. Diamonds from the Popigai impact structure, Russia. Geology 25:967–970.

Kumar, A.; Lin, P. A.; Xue, A.; Hao, B.; and Yap, Y. K.; and Sankaran, R. M. 2013. Formation of nanodiamonds at near-ambient conditions via microplasma dissociation of ethanol vapour. Nat. Commun. 4:2618.

Kurbatov, A. V.; Mayewski, P. A.; Steffensen, J. P.; West, A.; Kennett, D. J.; Kennett, J. P.; Bunch, T. E.; et al. 2010. Discovery of a nanodiamond-rich layer in the Greenland Ice Sheet. J. Glaciol. 56:747–757.

Kvasnytsya, V.; Wirth, R.; Dobrzhinetskaya, L.; Matzel, J.; Jacobsen, B.; Hutcheon, I.; Tappero, R.; and Kovalyukh, M. 2013. New evidence of meteoritic origin of the Tunguska cosmic body. Planet. Space Sci. 84:131–140.

Langenhorst, F.; Shafranovsky, G.; and Masaitis, V. L. 1998. A comparative study of impact diamonds from the Popigai, Ries, Sudbury, and Lappajärvi craters. Meteorit. Planet. Sci. 33:A90–A91.

LeCompte, M. A.; Goodyear, A. C.; Demitroff, M. N.; Batchelor, D.; Vogel, E. K.; Mooney, C.; Rock, B. N.; and Seidel, A. W. 2012. Independent evaluation of conflicting microspherule results from different investigations of the Younger Dryas impact hypothesis. Proc. Natl. Acad. Sci. USA 109:E2960–E2969.

Madden, A. S.; Swindle, A. L.; Bement, L. C.; Carter, B. J.; Simms, A. R.; and Benamara, M. 2012. Nanodiamonds and carbonaceous grains in Bull Creek Valley, Oklahoma. Mineral. Mag. 76(6):2051.

Mahaney, W. C.; Kalm, V.; Krinsley, D. H.; Tricart, P.; Schwartz, S.; Dohm, J.; Kim, K. J.; et al. 2010. Evidence from the northwestern Venezuelan Andes for extraterrestrial impact: the black mat enigma. Geomorphology 116:48–57.

Maruyama, K.; Makino, M.; Kikukawa, N.; and Shiraishi, M. 1992. Synthesis of hexagonal diamond in a hydrogen plasma jet. J. Mater. Sci. Lett. 11:116–118.

Meese, D. A.; Gow, A. J.; Alley, R. B.; Zielinski, G. A.; Grootes, P. M.; Ram, M.; Taylor, K. C.; Mayewski, P. A.; and Bolzan, J. F. 1997. The Greenland Ice Sheet Project 2 depth-age scale: methods and results. J. Geophys. Res. 102(C12):26,411–26,423.

Miura, Y., and Okamoto, M. 1997. Shocked metamor-

phosed materials from limestone by impacts. *In* Gorelli, R., ed. Antarctic meteorites XXI: papers presented to the 21st Symposium on Antarctic Meteorites. Tokyo, National Institute of Polar Research, p. 107–110.

Newman, J. D., and Herd, C. D. K. 2013. Whitecourt Meteorite Impact Crater: distribution, texture, and mineralogy of meteorites and the discovery of carbon spherules possibly associated with the impact event. Lunar and Planetary Science Conference, 44th (The Woodlands, TX, 2013), Abstract 2316.

Oleinik, G. S.; Valter, A. A.; and Erjomenko, G. K. 2003. The structure of high-pressure lonsdaleite diamond grains from the impactites of the Belilovka (Zapadnaja) astrobleme (Ukraine). Lunar and Planetary Science Conference, 34th (League City, TX, 2003), abstract 1561.

Paquay, F. S.; Goderis, S.; Ravizza, G.; Vanhaeck, F.; Boyd, M.; Surovell, T. A.; Holliday, V. T.; Haynes, C. V., Jr.; and Claeys, P. 2009. Absence of geochemical evidence for an impact event at the Bølling–Allerød/Younger Dryas transition. Proc. Natl. Acad. Sci. USA 106: 21,505–21,510.

Peng, J. L.; Orwa, J. O.; Jiang, B.; Prawer, S.; and Bursill, L. A. 2001. Nano-crystals of c-diamond, n-diamond and i-carbon grown in carbon-ion implanted fused quartz. Int. J. Mod. Phys. B 15:3107–3123.

Petaev, M. I.; Huang, S.; Jacobsen, S. B.; and Zindler, A. 2013. Large Pt anomaly in the Greenland ice core points to a cataclysm at the onset of Younger Dryas. Proc. Natl. Acad. Sci. USA 110:12,917–12,920.

Pinter, N.; Scott, A. C.; Daulton, T. L.; Podoll, A.; Koeberl, C.; Anderson, R. S.; and Ishman, S. E. 2011. The Younger Dryas impact hypothesis: a requiem. Earth Sci. Rev. 106:247–264.

Rasmussen, S. O.; Andersen, K. K.; Svensson, A. M.; Steffensen, J. P.; Vinther, B. M.; Clausen, H. B.; Siggaard-Andersen, M.-L.; et al. 2006. A new Greenland ice core chronology for the last glacial termination. J. Geophys. Res. 111(D6):D06102.

Redmond, B. G., and Tankersley, K. B. 2011. Species response to the theorized Clovis comet impact at Sheriden Cave, Ohio. Curr. Res. Pleistocene 28:141–143.

Reimer, P. J.; Bard, E.; Bayliss, A.; Beck, J. W.; Blackwell, P. G.; Bronk Ramsey, C.; Buck, C. E.; et al. 2013. IntCal13 and Marine13 radiocarbon age calibration curves 0–50,000 years cal BP. Radiocarbon 55:1869–1887.

Rösler, W.; Hoffmann, V.; Raeymaekers, B.; Schryvers, D.; and Popp, J. 2005. Diamonds in carbon spherules—evidence for a cosmic impact? Annual Meteoritical Society Meeting, 68th (Gatlinburg, TN, 2005), abstract 5114.

Rösler, W.; Hoffmann, V.; Raeymaekers, B.; Yang, Z. Q.; Schryvers, D.; and Tarcea, N. 2006. Carbon spherules with diamonds in soils. First International Conference on Impact Cratering in the Solar System (40th ESLAB Symposium; Noordwijk, Netherlands), Abstract 295464.

Santiago, P.; Camacho-Bragado, G. A.; Martin-Almazo, M.; Murgich, M.; and José-Yacaman, J. 2004. Diamond polytypes in Mexican crude oil. Energy Fuels 18:390–395.

Schoell, M., and Carlson, R. M. K. 1999. Diamondoids and oil are not forever. Nature 399:15–16.

Scott, A. C.; Pinter, N.; Collinson, M. E.; Hardiman, M.; Anderson, R. S.; Brain, A. P. R.; Smith, S. Y.; Marone, F.; and Stampanoni, M. 2010. Fungus, not comet or catastrophe, accounts for carbonaceous spherules in the Younger Dryas "impact layer." Geophys. Res. Lett. 37:L14302. doi:10.1029/2010GL043345.

Shelkov, D. A.; Verchovsky, A. B.; Milledge, H. J.; Kaminsky, F. V.; and Pillinger, C. T. 1998. Carbon, nitrogen, argon and helium study of impact diamonds from Ebeliakh alluvial deposits and Popigai crater. Meteorit. Planet. Sci. 33:985–992.

Steffensen, J. P.; Andersen, K. K.; Bigler, M.; Clausen, H. B.; Dahl-Jensen, D.; Fischer, H.; Goto-Azuma, K.; et al. 2008. High-resolution Greenland ice core data show abrupt climate change happens in few years. Science 321:680–684.

Su, Z.; Zhou, W.; and Zhang, Y. 2011. New insight into the soot nanoparticles in a candle flame. Chem. Commun 47:4700–4702.

Surovell, T. A.; Holliday, V. T.; Gingerich, J. A.; Ketron, C.; Haynes, C. V., Jr.; Hilman, I.; Wagner, D. P.; Johnson, E.; and Claeys, P. 2009. An independent evaluation of the Younger Dryas extraterrestrial impact hypothesis. Proc. Natl. Acad. Sci. USA 106:18,155–18,158.

Tian, H.; Schryvers, D.; and Claeys, P. 2011. Nanodiamonds do not provide unique evidence for a Younger Dryas impact. Proc. Natl. Acad. Sci. USA 108:40–44.

Van Geel, B.; Coope, G. R.; and Van der Hammen, T. 1989. Palaeoecology and stratigraphy of the lateglacial type section at Usselo (The Netherlands). Rev. Palaeobot. Palynol. 60:25–129.

van Hoesel, A.; Hoek, W. Z.; Braadbaart, F.; van der Plicht, J.; Pennock, G. M.; and Drury, M. R. 2012. Nanodiamonds and wildfire evidence in the Usselo horizon postdate the Allerød-Younger Dryas boundary. Proc. Natl. Acad. Sci. USA 109:7648–7653.

van Hoesel, A.; Hoek, W. Z.; Pennock, G. M.; and Drury, M. R. 2014. The Younger Dryas impact hypothesis: a critical review. Quat. Sci. Rev. 83:95–114.

Ward, G. K., and Wilson, S. R. 1978. Procedures for comparing and combining radiocarbon age determinations: a critique. Archaeometry 20:19–31.

Waters, M. R., and Stafford, T. W., Jr. 2007. Redefining the age of Clovis: implications for the peopling of the Americas. Science 315:1122–1126.

Welz, S.; McNallan, M. J.; and Gogotsi, Y. 2006. Carbon structures in silicon carbide derived carbon. J. Mater. Process. Technol. 179:11–22.

Wen, B.; Melnik, R.; Yao, S.; and Li, T. 2011. Hydrogen-doped cubic diamond and the crystal structure of n-diamond. Chem. Phys. Lett. 516:230–232.

Wen, B.; Zhao, J. J.; and Li, T. J. 2007. Synthesis and crystal structure of n-diamond. Inter. Mat. Rev. 52: 131–151.

Wittke, J. H.; Weaver, J. C.; Bunch, T. E.; Kennett, J. P.; Kennett, D. J.; Moore, A. M. T.; Hillman, G. C.; et al.

2013. Evidence for deposition of 10 million tonnes of cosmic impact spherules across four continents 12,800 y ago. Proc. Natl. Acad. Sci. USA 110:E2088–E2097.

Wolbach W. S. 1990. Carbon across the Cretaceous-Tertiary Boundary. PhD dissertation, University of Chicago.

Wu, Y.; Sharma, M.; LeCompte, M. A.; Demitroff, M.; and Landis, J. D. 2013. Origin and provenance of spher-

ules and magnetic grains at the Younger Dryas boundary. Proc. Natl. Acad. Sci. USA 110:E3557–E3566.

Yang, Z. Q.; Verbeeck, J.; Schryvers, D.; Tarcea, N.; Popp, J.; and Rösler, W. 2008. TEM and Raman characterization of diamond micro and nanostructures in carbon spherules from upper soils. Diam. Relat. Mater. 17: 937–943.